

# A Causal Exposure Response Function with Local Adjustment for Confounding

Georgia Papadogeorgou\* and Francesca Dominici

Department of Biostatistics, Harvard T.H. Chan School of Public Health, Boston MA 02115

## Abstract

In the last two decades, ambient levels of air pollution have declined substantially. Yet, as mandated by the Clean Air Act, we must continue to address the following question: is exposure to levels of air pollution that are well below the National Ambient Air Quality Standards (NAAQS) harmful to human health? Furthermore, the highly contentious nature surrounding environmental regulations necessitates casting this question within a causal inference framework.

Several parametric and semi-parametric regression modeling approaches have been developed for estimating the exposure-response (ER) curve. However, most of these approaches: 1) are not formulated in the context of a potential outcome framework for causal inference; 2) adjust for the same set of potential confounders across all levels of exposure; and 3) do not account for model uncertainty regarding covariate selection and shape of the ER. In this paper, we introduce a Bayesian framework for the estimation of a causal ER curve called LERCA (Local Exposure Response Confounding Adjustment). LERCA allows for: a) different confounders *and* different strength of confounding at the different exposure levels; and b) model uncertainty regarding confounders' selection and the shape of ER. Also, LERCA provides a principled way of assessing the observed covariates' confounding importance at different exposure levels.

We compare our proposed method with state of the art approaches in causal inference for ER estimation using simulation studies. We also apply the proposed method to a large data set that includes health, weather, demographic, and pollution for 5,362 zip codes and for the years of 2011-2013. An R package is available at <https://github.com/gpapadog/LERCA>.

*Keywords:* air pollution, cardiovascular hospitalizations, exposure response function, local confounding, particulate matter

---

\*Funding for this work was provided by National Institutes of Health R01 ES024332, USEPA 83587201-0, and Health Effects Institute 4953-RFA14-3/16-4.

## 1. Introduction

The Clean Air Act, one of the most comprehensive and expensive air quality regulations in the world, requires that we routinely address the following question: is exposure to levels of air pollution, even below the National Ambient Air Quality Standards (NAAQS), harmful to human health? As mandated by the Clean Air Act, if the peer reviewed literature reports consistent evidence of air pollution health effects, then the NAAQS must be lowered, even at the cost of hundreds of million of dollars. With the next review of the NAAQS for fine particulate matter ( $PM_{2.5}$ ) scheduled to be completed by the end of the year 2020, the determination of whether exposure levels of  $PM_{2.5}$  well below the NAAQS is harmful to human health is subject to unprecedented level of scrutiny. More recently, because of the highly contentious nature surrounding air pollution regulations and the lowering of the NAAQS particularly, there is an increasing pressure to cast this question within a causal inference framework [Zigler and Dominici, 2014]. The methods development in this paper is motivated by the need to address this critically important question, by developing an approach that flexibly estimates an exposure response curve while reliably eliminating confounding bias especially at low levels of exposure.

The literature on the harmful effects of air pollution is very extensive [Dominici et al., 2002, Eftim et al., 2008, Zeger et al., 2008, Zanobetti and Schwartz, 2007, Di et al., 2017a,b, Berger et al., 2017], but significant substantive and methodological gaps remain, especially in the context of estimating health effects at very low levels of exposure. Parametric and semi-parametric regression modelling approaches for ER estimation have been proposed in the literature in the context of clinical trials data [Babb et al., 1998], toxicology [Scholze et al., 2001], and air pollution research [Bell et al., 2006, Daniels et al., 2000, Dominici et al., 2002, Schwartz et al., 2002, Shi et al., 2016]. Regression and semi-parametric modeling approaches for ER estimation such as Generalized Linear Models or Generalized Additive Models [Hastie and Tibshirani, 1986, Daniels et al., 2004, Shaddick et al., 2008, Shi et al., 2016, Dominici et al., 2002], generally make the following assumptions: 1) the same potential confounders are considered when estimating the health effects across all exposure levels (i.e. global confounding adjustment); 2) the set of potential confounders that are included into the regression model among a potentially large set of available covariates is specified a priori; 3) these pre-selected potential confounders are included into the model as linear or spline terms for confounding adjustment (i.e. parametric/semi-parametric adjustment for confounding bias); and 4) the shape of the ER function is modelled as a spline, a polynomial, or linear with a threshold.

In the causal inference literature, Hirano and Imbens [2004] introduced the generalized propensity score (GPS) in order to adjust for confounding when estimating the causal effects of a continuous exposure. More recently, Kennedy et al. [2017] introduced a doubly robust approach for estimating the causal ER function using flexible machine learning tools, and derived groundbreaking theory for the estimator’s asymptotic performance. These approaches are really promising and manifest the growing interest in principled causal inference methods for continuous exposures. However, they still rely on global confounding adjustment of pre-selected potential confounders, and do not provide guidance of the covariates’ confounding importance at different exposure levels.

In our exploratory analyses (§2), we report that the relationship between exposure to  $PM_{2.5}$  and health outcome (rate of hospitalization for cardiovascular diseases) might be confounded by a *different set of covariates* at the low exposure levels versus at the high exposure levels and also that the amount of confounding bias varies greatly across the exposure levels. We refer to this phenomenon as *local confounding*. In simulation studies, we will illustrate that when local confounding is present, state of the art approaches for estimating ER are biased. We argue that –especially in the context of estimating causal effects at low levels of exposure– local confounding adjustment is deemed necessary.

To target local confounding, one could adopt a separate model at each exposure level flexibly

adjusting for all the available potential confounders. However, including unnecessary confounders could lead to inefficient estimation of causal effects, especially at very low levels of exposure. Data driven methods to select the minimum necessary set of covariates to be included into an outcome model for estimation of causal effects have been proposed [Luna et al., 2011, Wang et al., 2012, Wilson and Reich, 2014], but to our knowledge, they have not been developed further in the context of ER estimation to achieve local confounding adjustment.

Furthermore, although parametric or semi-parametric modelling of the ER are attractive for their flexibility in identifying different shapes (see for example Dominici et al. [2002], Daniels et al. [2000], Scholze et al. [2001], Schwartz et al. [2002], Govindarajulu et al. [2009], Shaddick et al. [2008]), they heavily rely on model specification and borrowing of information across exposure levels. Another challenge is that smooth functions (such as splines) do not allow for a hockey stick shape of ER curve, which is one of our key epidemiological questions.

The goal of this paper is to overcome the challenges described above by introducing a Bayesian framework for the estimation of a causal ER curve called LERCA (Local Exposure Response Confounding Adjustment). We cast our approach within a causal inference framework by introducing the concept of *experiment configuration*  $\mathbf{s} = (s_0, s_1, \dots, s_{K+1})$ , where  $[s_{k-1}, s_k)$  denotes a specific range of exposure values. We use the term *experiment* to mimic the hypothetical assignment of a unit to exposure value within  $[s_{k-1}, s_k)$ . Within each experiment, i.e. *locally* in the exposure range  $[s_{k-1}, s_k)$ , we assume that: 1) ER is linear; and 2) the potential confounders of the exposure-outcome relationship are unknown but observed; and 3) the strength of the local confounding is also unknown. Importantly, the *experiment configuration*  $\mathbf{s}$  is itself unknown and it will be estimated from the data.

In §2 we introduce the dataset, and we use our data to illustrate the issue of local confounding. In §3, we introduce the notation and assumptions. In §4 we introduce our approach, and in §5 we compare it with alternative methods in the presence of local or global confounding through extensive simulations. Finally, we apply LERCA to estimate the causal ER function of long term exposure to PM<sub>2.5</sub> on Medicare log cardiovascular hospitalization rates in §6. Limitations and potential extensions are discussed in §7.

## 2. Data description and illustration of local confounding

In this section we illustrate that, in our data set, some covariates are highly imbalanced at low exposure levels whereas others are highly imbalanced at the high exposure levels. Our methods development is motivated to overcome this particular challenge. We assemble a data set where the unit of the observation is the zip code  $i$ , with sample size  $N = 5,362$ . For each zip code, we calculate: the exposure  $X_i$  defined as the average of daily levels of PM<sub>2.5</sub> for the years 2011 and 2012 recorded by monitors within 6 mile radius of zip code  $i$ 's centroid. The values of  $X_i$  range from 2.7 to  $18.3\mu\text{g}/\text{m}^3$  (see also Figure 1). We also acquired information on several potential confounders, denoted by  $C_{ij}$  for  $j = 1, 2, \dots, p$  and  $p = 27$ , capturing socio-economic, demographic, climate, and risk factor information for these zip codes. Appendix A includes additional information regarding this data set.

In order to illustrate the potential of local confounding in our data we considered two subsets of zip codes: 1) zip codes with low exposure ( $3 - 8\mu\text{g}/\text{m}^3$ ; 816 observations); and 2) zip codes with high exposure ( $12 - 13\mu\text{g}/\text{m}^3$ ; 324 observations). For each of these two subsets of zip codes, we introduce a binary treatment ( $T_{i1}$  and  $T_{i2}$ ) defined as follows:

1.  $T_{i1} = 0$  if  $3 < X_i \leq 7$ , low exposure within the low exposure subset,
2.  $T_{i1} = 1$  if  $7 < X_i \leq 8$ , high exposure within the low exposure subset,

3.  $T_{i2} = 0$  if  $12 < X_i \leq 12.5$ , low exposure within the high exposure subset, and
4.  $T_{i2} = 1$  if  $12.5 < X_i \leq 13$ , high exposure within the high exposure subset.

In other words, we introduce two binary treatment indicators  $T_{i1}$  and  $T_{i2}$ , one in the low and the other in the high exposure group. Separately for these two subsets of zip codes, and for each covariate  $C_{ij}$ , we calculate the absolute standardized difference of means (ASDM). Figure 2 shows ASDM when comparing zip codes with  $T_{i1} = 1$  versus  $T_{i1} = 0$  (blue triangles for the low exposure group) and when comparing zip codes with  $T_{i2} = 1$  versus  $T_{i2} = 0$ , separately (red circles for the high exposure group). Visual inspection of Figure 2 indicates presence of *local confounding*, that is,

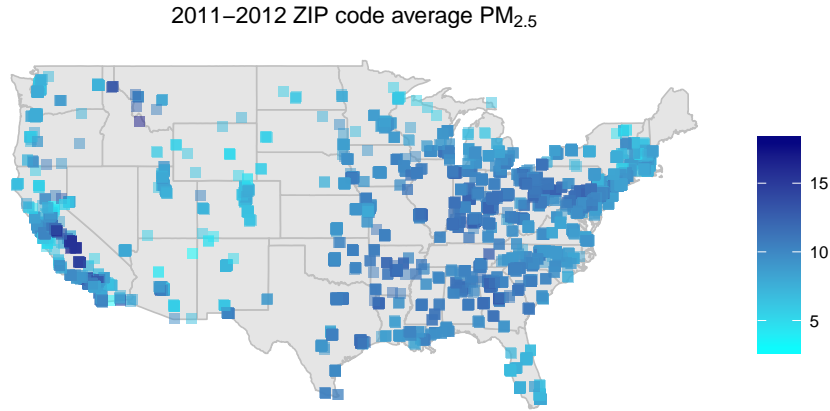


Figure 1: Average levels of  $PM_{2.5}$  for the years 2011-2012 for each zip code  $i$  included into the analysis.

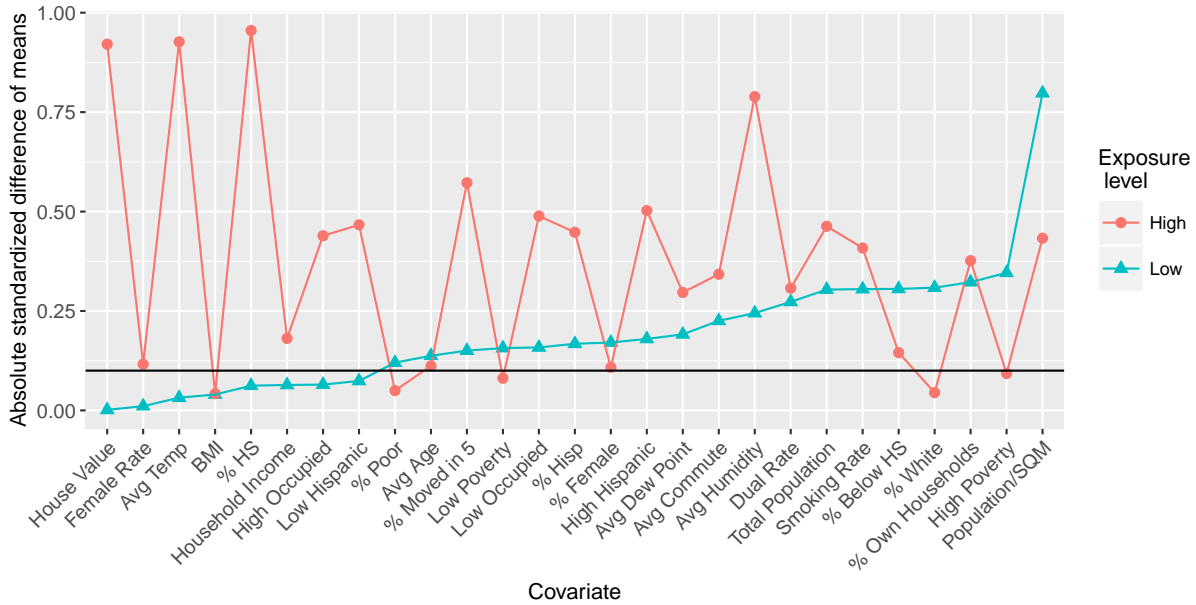


Figure 2: Absolute standardized difference of means (ASDM) of each potential confounder. The ASDM is calculated separately for two subsets of zip codes, the ones at low exposure (blue) and the ones at high exposure (red). Covariates are ordered with respect to ASDM values for the zip codes at low exposure.

different variables are imbalanced at the low versus the high exposure levels. For example, median house value (in logarithm – `House Value`) is highly imbalanced when considering zip codes at higher exposure values, whereas is not when considering zip codes at lower levels. The opposite is true for other variables such as the proportion of population that is white (`% White`), or has less than high school education (`% Below HS`).

### 3. Notation and Assumptions

We follow the potential outcome framework [Neyman, 1923, Rubin, 1974, Hirano and Imbens, 2004], and under the assumptions of SUTVA; no interference, no hidden versions of the treatment [Rubin, 1980], we denote  $Y_i(x)$  to be the potential outcome for observation  $i$  at exposure  $x \in \mathcal{X}$ , where  $\mathcal{X}$  is the interval on the real line of all possible exposure values. Let  $\{Y_i(x), x \in \mathcal{X}\}$  be the individual ER curve, and  $\{\bar{Y}(x) = E[Y_i(x)], x \in \mathcal{X}\}$  the population average ER curve. Assuming sufficient smoothness of  $\bar{Y}(x)$  as a function of  $x$ , we define the instantaneous causal effect

$$\Delta(x) = \lim_{h \rightarrow 0} \frac{\bar{Y}(x+h) - \bar{Y}(x)}{h}.$$

A  $\Delta(x) \neq 0$  implies that variation in the exposure in a neighborhood of  $x$  has a causal effect on the expected outcome. We also define the population average causal effect of an exposure shift from  $x$  to  $x + \delta$ , as  $CE_\delta(x) = \bar{Y}(x + \delta) - \bar{Y}(x) = \int_x^{x+\delta} \Delta(t) dt$ .

The observed values of the exposure and the  $p$  measured covariates for observation  $i$  are denoted as  $X_i$  and  $\mathbf{C}_i = (C_{i1}, C_{i2}, \dots, C_{ip})$  accordingly. Then, the observed outcome  $Y_i$  is equal to the potential outcome at the observed exposure  $Y_i(X_i)$ .

**3.1 Experiment configuration, global and local ignorability assumption** The weak ignorability assumption for a continuous exposure [Hirano and Imbens, 2004] states that the treatment is as if randomized conditional on observed covariates

$$X \perp\!\!\!\perp Y(x) | \mathbf{C}, \quad x \in \mathcal{X}, \tag{1}$$

and every subject in the population can experience any  $x \in \mathcal{X}$ . Consider a minimal confounding adjustment set  $\mathbf{C}^* \subseteq \mathbf{C}$  such that  $X \perp\!\!\!\perp Y(x) | \mathbf{C}^*, x \in \mathcal{X}$ . Such sets have been previously discussed in the literature [Luna et al., 2011, Wang et al., 2012, Vansteelandt et al., 2012], and they are such that the independence assumption in (1) does not hold for any strict subset of  $\mathbf{C}^*$ .

In this paper we are interested in overcoming the situation where the minimal sufficient adjustment set  $\mathbf{C}^*$  might vary across exposure levels. We formalize this by introducing the *experiment configuration*. Let  $K$  denote a fixed positive integer,  $\min = \min x_i$  and  $\max = \max x_i$  the minimum and maximum values of the exposure range  $\mathcal{X}$ , and  $\bar{s} = (s_0 = \min, s_1, s_2, \dots, s_K, s_{K+1} = \max)$  a known partition of the exposure range in  $K + 1$  experiments  $g_k = [s_{k-1}, s_k), k = 1, 2, \dots, K + 1$ . In Figure 3, a hypothetical exposure response function is plotted where  $\bar{s}$  defines a total of 4 experiments ( $K = 3$ ). Then, a minimal sufficient adjustment set  $\mathbf{C}^*$  can be written as  $\mathbf{C}^* = \cup_{k=1}^{K+1} \mathbf{C}_k^*$ , where  $\mathbf{C}_k^*$  is a minimal sufficient adjustment set for treatment assignment in experiment  $k$ , and therefore satisfies

$$X \perp\!\!\!\perp Y(x) | \mathbf{C}_k^*, \quad x \in g_k. \tag{2}$$

The sets  $\mathbf{C}_k^*$  can be overlapping (or even identical) if the same variable is necessary for confounding adjustment at more than one experiment. Note that if (2) is satisfied, then (1) is also satisfied.

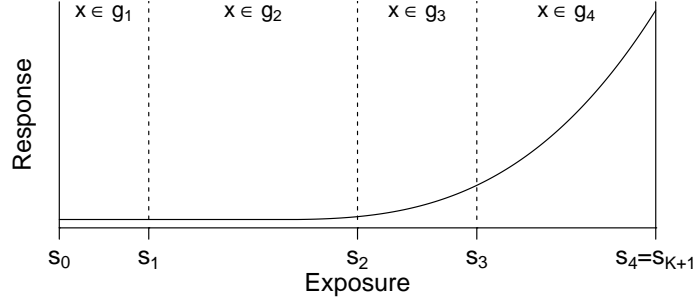


Figure 3: Hypothetical ER curve. The exposure range is partitioned by  $\bar{s}$  in 4 experiments.

Given  $\bar{s}$  and assuming sets  $\mathbf{C}_k^*$  satisfying (2), model choice can be performed locally within each experiment  $g_k$ . Thus, local model selection allows for the identification and adjustment for a different set of confounders at different exposure levels.

#### 4. ER estimation in the presence of local confounding

In §4.1 and §4.2 we introduce LERCA (Local Exposure Response Confounding Adjustment) for a fixed and for an unknown experiment configuration, respectively. The choice of  $K$  for the unknown experiment configuration is discussed in §4.4.

**4.1 Known experiment configuration** Locally, that is for  $x \in g_k$ ,  $k = 1, 2, \dots, K + 1$ , we assume the following pair of exposure and outcome models:

$$\begin{aligned}
 p(x|\mathbf{C} = \mathbf{c}, x \in g_k) &\propto \phi(x; \delta_{k0}^X + \sum_{j=1}^p \alpha_{kj}^X \delta_{kj}^X c_j, \sigma_{k,X}^2) \\
 p(y|X = x, \mathbf{C} = \mathbf{c}, x \in g_k) &= \phi(y; \delta_{k0}^Y + \beta_k(x - s_{k-1}) + \sum_{j=1}^p \alpha_{kj}^Y \delta_{kj}^Y c_j, \sigma_{k,Y}^2)
 \end{aligned} \tag{3}$$

where  $\phi(\cdot; \mu, \sigma^2)$  denotes the normal density with mean  $\mu$  and variance  $\sigma^2$ ,  $\alpha_{kj}^X = 1$  indicates that covariate  $C_j$  is included into the exposure model of the  $k^{\text{th}}$  experiment, and  $\alpha_{kj}^X = 0$  is not. The parameter  $\alpha_{kj}^Y$  has the same interpretation, but for the outcome model. The parameter  $\beta_k$  denotes the instantaneous change in the expected outcome associated with a local variation in exposure for  $x \in g_k$ . Model (3) allows for a different set of variables and variables' coefficients at the different experiments. (Note that the coefficients and variance terms depend on the inclusion indicators of the corresponding model. For notational simplicity, we do not explicitly state this dependence.) If the minimal confounding adjustment set for experiment  $k$  is included in the outcome model and the mean functional form is correctly specified,  $\beta_k$  is an unbiased estimator of the instantaneous effect  $\Delta(x)$ , for  $x \in g_k$ . The assumption of local linearity (linear effect of the exposure on the outcome within each experiment) can lead to global non-linearity, and can be easily relaxed, as discussed in §7.

Below we discuss how the prior distributions are chosen to target confounding adjustment and continuous ER estimation. More details on the prior specifications can be found in Appendix B.

**4.1.1 Prior distribution on inclusion indicators for confounding adjustment** We build upon the work by Wang et al. [2012, 2015] to assign an informative prior on covariates' local inclusion indicators  $(\alpha_{kj}^X, \alpha_{kj}^Y)$ . This prior choice ensures that model averaging assigns high posterior weights to outcome

models including a minimal confounding adjustment set separately for each exposure range, and specifies

$$\frac{P(\alpha_{kj}^Y = 1 | \alpha_{kj}^X = 1)}{P(\alpha_{kj}^Y = 0 | \alpha_{kj}^X = 1)} = \omega \text{ where } \omega > 1, \text{ iid } \forall j, k. \quad (4)$$

By specifying (4), a variable  $C_j$  is assigned high prior probability to be included into the outcome model if it is also included in the exposure model ( $x \in g_k$  &  $\alpha_{kj}^X = 1$ ). Wang et al. [2012] and Antonelli et al. [2017b] show that this informative prior leads to outcome models that include the minimal set of true confounders with higher posterior weights than model selection approaches that are based solely on the outcome model. In our context, this experiment-specific prior specification ensures that, locally, covariates in the minimal set  $\mathbf{C}_k^*$  are included in the outcome model of experiment  $k$  with high posterior probability.

*4.1.2 Prior distribution on outcome model intercepts and coefficients of exposure for ER continuity* If the covariates  $C_j$  are centered to have mean 0, continuity of the estimated ER function is ensured by assuming a point-mass recursive prior on the outcome model intercepts  $\delta_{k0}^Y, k \geq 2$ . That is,

$$\lim_{x \rightarrow s_k^+} E[Y|X = x] = \lim_{x \rightarrow s_k^-} E[Y|X = x] \iff \delta_{k0}^Y = \delta_{(k-1)0}^Y + \beta_{k-1}(s_k - s_{k-1}). \quad (5)$$

In other words, the outcome model intercept of experiment  $k \geq 2$  is a deterministic function of the outcome model intercept of the first experiment  $\delta_{10}^Y$ , and slopes  $\beta_1, \beta_2, \dots, \beta_{k-1}$ . These parameters are assigned independent non-informative normal prior distributions.

*4.1.3 Prior distributions of the remaining coefficients* Prior distributions on the remaining regression coefficients (exposure model coefficients, outcome model covariates' coefficients) and variance terms are chosen such that they lead to known forms of the full conditional posterior distributions to simplify the sampling. We assume independent non-informative Inverse Gamma prior distributions on  $\sigma_{k,X}^2, \sigma_{k,Y}^2$ . Non-informative normal prior is chosen for the exposure model intercept  $\delta_{k0}^X$ . Conditional on the inclusion indicators, the prior on the regression coefficient  $\delta_{kj}^Y$  is a point mass at 0, or a non-informative normal distribution when  $\alpha_{kj}^Y$  is equal to 0 or 1 accordingly. Similarly for the exposure model covariates' coefficients  $\delta_{kj}^X$ .

**4.2 Unknown experiment configuration** For a fixed experiment configuration  $\bar{\mathbf{s}}$ , each experiment is treated separately in terms of confounder *selection and strength* of the confounding adjustment. However, the configuration itself is a key component of the fitted exposure response curve, and fixing it a priori could lead to bias and uncertainty underestimation. In this section, we present LERCA in the context of an unknown experiment configuration  $\bar{\mathbf{s}}$ . More specifically, the locations of the experiment configuration  $\mathbf{s} = (s_1, s_2, \dots, s_K)$  are a priori assumed to be distributed as the even-numbered order statistics of  $2K + 1$  samples from a uniform distribution on the interval  $(s_0, s_{K+1})$ . This prior choice of  $\mathbf{s}$  discourages specifications of  $\mathbf{s}$  that include values that are too close to each other [Green, 1995]. The prior is augmented by indicators that consecutive points  $s_k, s_{k+1}$  cannot be closer than some distance  $d_k$ . Conditional on  $\mathbf{s}$ , we follow the model specification and prior distributions described in §4.1.

**4.3 MCMC scheme and convergence diagnostics** Markov Chain Monte Carlo methods (MCMC) are used to acquire samples from the posterior distribution, on which inference of quantities of interest is based. A detailed description of the MCMC scheme including computational challenges and contributions can be found in Appendix C. In the same section, we discuss MCMC convergence diagnostics based on the potential scale reduction factor (PSR; Gelman and Rubin [1992]) for quantities that do not directly depend on the experiment configuration.

**4.4 Choosing the number of points in the experiment configuration** LERCA requires the specification of the number of points  $K$  in the experiment configuration. Since the number of parameters grows with  $K$ , possible values for  $K$  could be bounded by considering the maximum number of coefficients we are willing to entertain.

Cross validation methods to choose values of tuning parameters are most often infeasible in the Bayesian framework due to time and computational resources constraints. In a comprehensive review, Gelman et al. [2014] discusses various methods of estimating the expected out of sample prediction error for Bayesian methods. The widely-applicable information criterion (WAIC; Watanabe [2010]) can be used to obtain an estimate of the out-of-sample prediction error based on one MCMC run. Specifically, LERCA is fit once for different values of  $K$ , and  $K$  is chosen as the value that minimizes the  $WAIC = -2(\text{lppd} - p_{WAIC})$ , where  $\text{lppd}$  and  $p_{WAIC}$  denote the log point-wise posterior predictive density and the penalty:

$$\begin{aligned} \text{lppd} &= \sum_{i=1}^n \log E_{\text{post}} p(x_i, y_i | \theta) \\ p_{WAIC} &= \sum_{i=1}^n \text{var}_{\text{post}} (\log p(x_i, y_i | \theta)) \end{aligned}$$

where  $\theta$  denotes the full vector of all the unknown parameters  $(\mathbf{s}, \boldsymbol{\alpha}^X, \boldsymbol{\alpha}^Y, \boldsymbol{\beta}, \boldsymbol{\delta}^X, \boldsymbol{\delta}^Y, \boldsymbol{\sigma}_X^2, \boldsymbol{\sigma}_Y^2)$  and  $E_{\text{post}}, \text{var}_{\text{post}}$  denote the posterior mean and variance.

## 5. Simulation Studies

**5.1 Data generation** In this section we generate data with local confounding and a quadratic ER. Details on the data generating mechanism are in Appendix D. We assume that exposure values range from 0 to 10, and the true experiment configuration is  $\bar{\mathbf{s}} = (0, 2, 4, 7, 10)$ . Table 1 summarizes which of the 8 potential confounders are predictive of the exposure and/or the outcome within each experiment (correlations and regression coefficients are summarized in Table E.1). We simulate 400 data sets of 800 observations each with exposure values uniformly sampled over the exposure range.

**5.2 Goal of the simulations** We illustrate that commonly-used and flexible approaches for ER estimation are not appropriate for confounding adjustment in the presence of local confounding. Approaches for ER estimation are fit using the `gam` and `causaldrf` R packages [Hastie, 2017, Schafer, 2015] as well as the code available on Kennedy et al. [2017]. Specifically we compare our approach to the following methods for estimation of ER:

1. Generalized Additive Model (**GAM**): Regressing the outcome  $Y$  on flexible functions of the exposure  $X$  and all potential confounders (4 degrees of freedom for each predictor).
2. Spline Model (**SPLINE**): Additive spline estimator described in Bia et al. [2014]. The generalized



Table 1: Representation of which covariates are predictive of the exposure and / or the outcome within each experiment (denoted by a  $\checkmark$ ). Covariates with  $\checkmark$  in both models within the same experiment are local confounders.

Experiment	Model	$C_1$	$C_2$	$C_3$	$C_4$	$C_5$	$C_6$	$C_7$	$C_8$
1	$X \mathbf{C}$	$\checkmark$	$\checkmark$	$\checkmark$					
	$Y X, \mathbf{C}$	$\checkmark$	$\checkmark$	$\checkmark$					
2	$X \mathbf{C}$	$\checkmark$	$\checkmark$		$\checkmark$				
	$Y X, \mathbf{C}$		$\checkmark$	$\checkmark$	$\checkmark$				
3	$X \mathbf{C}$	$\checkmark$		$\checkmark$		$\checkmark$			
	$Y X, \mathbf{C}$		$\checkmark$	$\checkmark$		$\checkmark$			
4	$X \mathbf{C}$		$\checkmark$			$\checkmark$	$\checkmark$		
	$Y X, \mathbf{C}$		$\checkmark$	$\checkmark$			$\checkmark$		

propensity score (gps) is modelled as a linear regression on all covariates. Then, the ER function is estimated using additive spline bases of the exposure and gps.

3. The Hirano and Imbens estimator [Hirano and Imbens, 2004] (HI-GPS): ER estimation is obtained by fitting an outcome regression model including quadratic terms for both the exposure and the gps, and the exposure-gps interaction. The gps is estimated as in SPLINE.
4. Inverse Probability Weighting estimator (IPW): The generalized propensity score is used to weigh observations in an outcome regression model that includes linear and quadratic terms of exposure. The gps is estimated as in SPLINE.
5. The doubly-robust approach of Kennedy et al. [2017] (KENNEDY): The gps and outcome models are estimated using the Super Learner algorithm [Van Der Laan et al., 2007] combining the sample mean, linear regression without and with two-way interactions, generalized additive models, multivariate adaptive regression splines and random forests. Based on the gps and outcome model estimates, the pseudo-outcome is calculated and is regressed on the exposure using kernel smoothing. This approach is chosen to represent state-of-the-art methods in ER estimation that are based on flexible, machine-learning and non-parametric approaches.

Using each method, we estimate the population average ER curve  $\bar{Y}(x)$ . We also calculate and compare the root mean squared error (rMSE) across the methods. Finally, we also assess whether LERCA can recover the correct experiment configuration, identify the true confounders within each experiment, and choose the true value for  $K$ .

**5.3 Simulation Results** For every simulated data set, LERCA was fit for  $K \in \{2, 3, 4\}$ , and the ER was estimated over an equally spaced grid of points over the interval  $(0, 10)$  denoted by  $\mathcal{G}$ . Note that in this data generating mechanism the minimal set of confounders vary across the four experiments, as evident by Table 1. Results are presented for the simulated data sets for which the MCMC converged for all choices of  $K$  (for convergence diagnostics, see Appendix C.3;  $c = 0.05$ ).

In Figure 4 we summarize the LERCA results including the estimated ER, and posterior distribution of the experiment configuration and outcome model inclusion indicators of covariates  $C_1, C_4$  as a function of exposure  $x \in (0, 10)$ . We choose  $C_1$  and  $C_4$  because, in this data generating mechanism,  $C_1$  is a necessary confounder in experiment 1 ( $x < 2$ ), and  $C_4$  is a necessary confounder in experiment 2 only ( $2 < x < 4$ ). Figure 5 shows the estimated ER curve under the alternative

methods described above. Grey lines correspond to results from individual data sets, whereas black solid lines correspond to averages across simulated data sets.

As showed in Figure 4, even though the true ER is quadratic and LERCA is formulated as piece-wise linear, LERCA is able to identify the correct shape of the exposure-response function. The alternative methods return biased results across the exposure range (as shown in Figure 5), especially at very low or very high levels of exposure. Indeed, we found that root MSE of LERCA was consistently lower than the alternative methods at low exposure levels (Figure E.1).

We also found that using WAIC to choose the value of  $K$  led to choosing the correct value of  $K = 3$  40% of the times, and  $K = 2$  58% of the times indicating that WAIC tends to penalize large values of  $K$ . Regardless, the correct points of the experiment configuration  $\mathbf{s} = \{2, 4, 7\}$  are identified and are located at the modes of the posterior distribution as shown in Figure 4. By examining the posterior inclusion probabilities of  $C_1, C_4$ , we observe that instrumental variables (e.g.,  $C_1$  in experiments 2 and 3) are often included in the outcome model. However, LERCA includes the minimal confounding set within each experiment with very high probability. On average (across the points in the exposure range and across all the simulated data sets) the minimal confounding set was included in the adjustment set 99% of the times (ranging from 89-100% across simulated data sets), indicating that the variables necessary for confounding adjustment are almost always

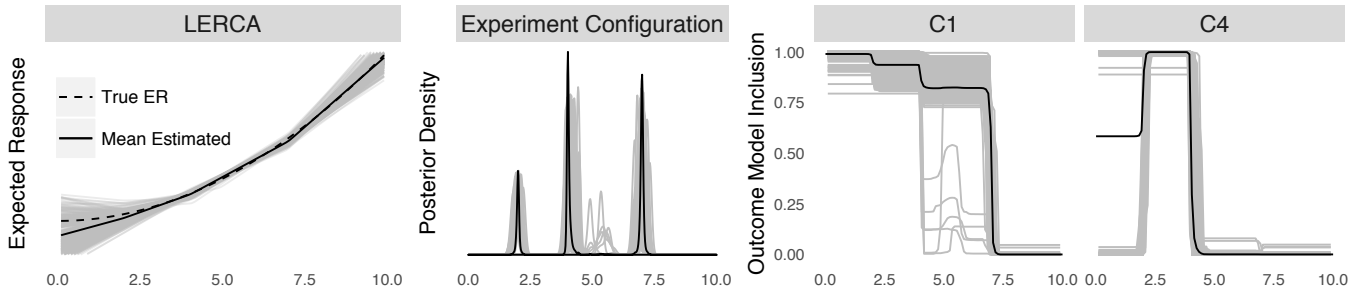


Figure 4: LERCA results. (Left) Mean ER estimates. (Center) Posterior density distribution of the experiment configuration  $\mathbf{s}$ . (Right) Outcome model posterior inclusion probability of  $C_1$  and  $C_4$ . Gray lines correspond to results per simulated data set, and black solid lines correspond to summaries across data sets.

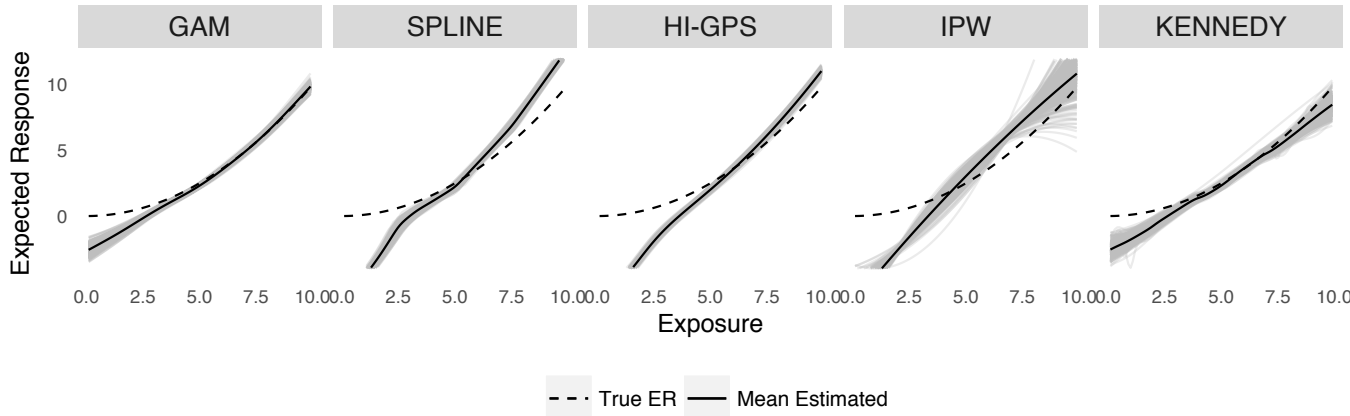


Figure 5: The true mean ER function (dashed line), estimated ER functions from each simulated data set (gray), and the mean of the estimated ER functions (solid lines) using all alternative methods.

included in the adjustment set. Lastly, the point-wise 95% and 50% credible intervals cover the true mean ER values 84% and 39% of the times accordingly. The under-coverage is largely due to the underestimation of  $K$ .

**5.4 Simulation results in the absence of local confounding** The previous data simulation scenario compared the performance of LERCA in the presence of local confounding. In Appendix E.2, LERCA is also compared to the other methods in the more traditional setting of global confounding, that is, in the setting more favorable to the alternative methods. In this context, LERCA with  $K = 3$  (fixed) performed similarly in terms of root MSE compared to GAM and Kennedy’s doubly-robust estimator, but better than the remaining alternative methods. These results indicate that LERCA offers a protection against bias arising from local confounding, without sacrificing efficiency when local confounding is not present.

## 6. Data Application

In this section, LERCA is applied to the data set introduced in §2. Our goal is to estimate the causal relationship between  $x_i$  (average exposure to  $PM_{2.5}$  for the years 2011-2012) and  $y_i$  (log cardiovascular hospitalization rates in 2013). The full set of zip code level covariates are described in Table A.1. We allow  $K$  to take values  $\{2, 3, \dots, 6\}$  and we report the results for  $K = 3$  which corresponds to the lowest WAIC.

Figure 6 shows (a) posterior mean and the 95% credible intervals of the ER; (b) posterior mean and 95% credible interval of  $\beta_k$  (positive values imply that an increase in  $PM_{2.5}$  exposure lead to an increase in hospitalization rates), (c) the posterior distribution of the experiment configuration, and (d) the observed distribution of  $PM_{2.5}$ .

We found statistically significant evidence that small increases in exposure are associated with increases in log hospitalization rates for exposure values lower than  $9.9\mu g/m^3$ , but this evidence loses significance for values of  $x \geq 9.9\mu g/m^3$ . Note that the current NAAQS for long term exposure to  $PM_{2.5}$  are equal to  $12\mu g/m^3$ . These results are consistent with other epidemiological studies which have found that the strength of the association between long term exposure to  $PM_{2.5}$  on health outcomes is larger at low exposure levels [Dominici et al., 2002, Di et al., 2017b]. Lastly, the posterior distribution of  $\mathbf{s}$ , shows that observations below  $8\mu g/m^3$  and over  $11.5\mu g/m^3$  are always grouped together.

As done in the simulation study, the covariates’ posterior inclusion probability can be plotted as a function of the exposure values. Figure 7 shows the posterior exposure and outcome model inclusion probability for three covariates. The posterior inclusion probabilities vary substantially as a function of the exposure indicating that local confounding is present. It is worth noting that for most variables, the posterior inclusion probability depicted in Figure 7 agree with the initial covariate balance shown in Figure 2. For example, in both cases the covariate corresponding to median house value is a predictor of exposure at high exposure levels, while it’s not predictive of exposure at low exposure levels.

## 7. Discussion

We have introduced an innovative Bayesian approach for flexible estimation of the ER curve in observational studies that has the following important features: 1) it casts the formulation of the ER within a potential outcome framework, and we mimic several randomized experiments across exposure levels; 2) let the data inform the experiment configuration; and given the current experiment

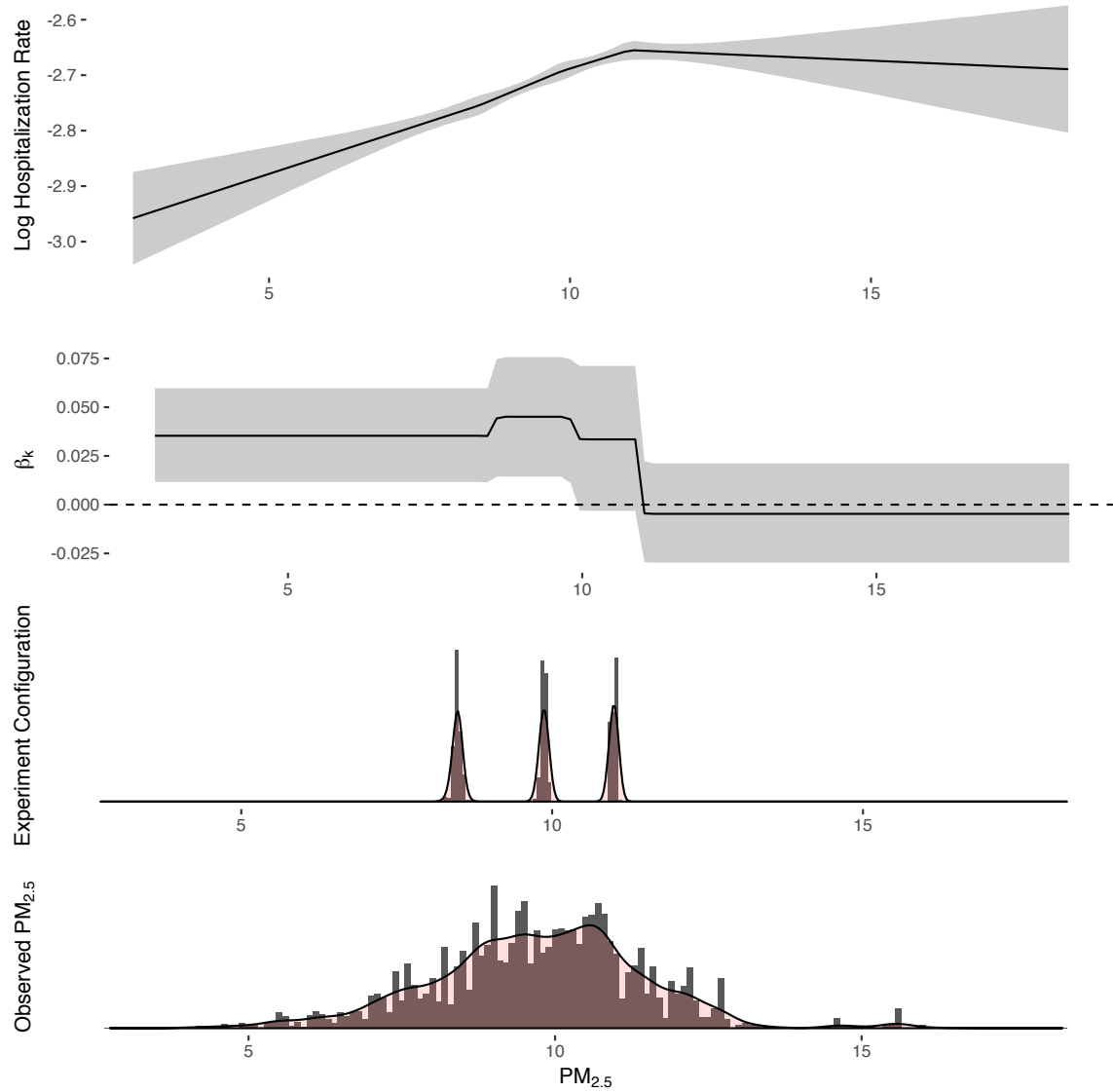


Figure 6: From top to bottom: Mean ER curve of  $PM_{2.5}$  exposure (x-axis) and log all-cause cardiovascular hospitalizations (y-axis) –solid line– with 95% pointwise credible intervals. The posterior mean and 95% credible interval of the  $\beta$  coefficient as a function of exposure. The posterior distribution for  $s$  for  $K = 3$ . Observed  $PM_{2.5}$  values in the data.

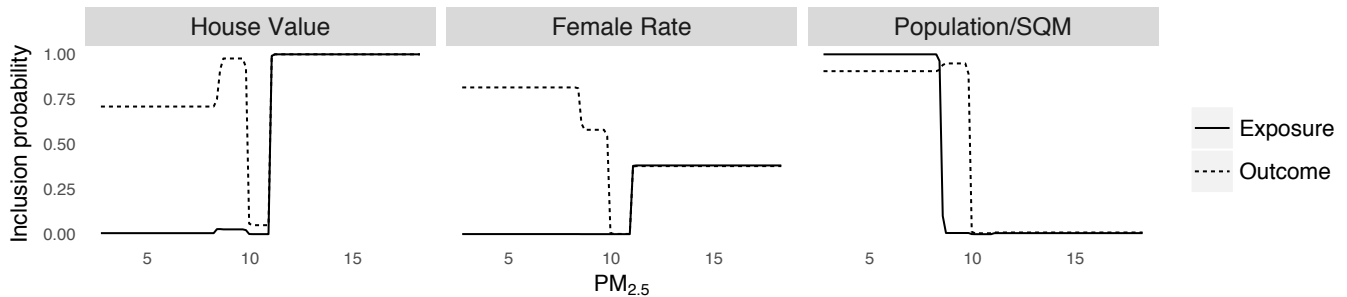


Figure 7: Posterior inclusion probability of zip code median house value, Medicare female rate, and population density in the exposure and outcome model at different exposure levels.

configuration 3) allows for the possibility which is a reality in our data example (Figure 2 and Figure 7) that different sets of covariates are indeed confounders at different exposure levels; 4) allows for varying confounding effect across levels of the exposure; 5) performs local covariate selection, thus increasing efficiency, especially at low exposure levels; 6) propagates model uncertainty for the experiment configuration and covariate selection in the posterior inference on the whole ER curve; and finally, 7) provides important scientific guidance related to which covariates are confounders at different exposure levels.

The main contribution of this paper is in addressing the issue of local confounding in ER estimation, and in providing evidence of covariates' confounding importance at different exposure levels. In doing so, LERCA is based on several modeling and other decisions that can be easily altered, such as local linearity in the exposure and outcome models, the prior specification of covariates' inclusion indicators for confounding adjustment, and the MCMC approach to acquire samples from the posterior distribution of all parameters. Some of these decisions are criticized below, and how to optimize LERCA in different scenarios is an interesting line of future research.

First, within each experiment and thus locally within a narrow exposure range, we assume linearity for both the outcome and the exposure model. Local linearity could be easily relaxed by using higher order splines. In simulation studies where the true ER is quadratic, LERCA does recover the true non linear shape. An interesting line of research is to fully explore the robustness of the LERCA performance to the assumption of local linearity for confounding adjustment, as well as extensions accommodating flexible functions.

Second, the informative prior on the inclusion indicators could lead to the inclusion of instrumental variables in the outcome model, which will not lead to bias, but will decrease the efficiency of our estimators. However, in the study of air pollution, strong instrumental variables are not expected to be present. Alternative strategies for local covariate selection for confounding adjustment can be accommodated here, extending, for example, work by [Wilson and Reich \[2014\]](#), [Cefalu et al. \[2017\]](#), [Antonelli et al. \[2018\]](#). Further work could evaluate the performance of different approaches to model selection (via prior specifications or penalization techniques) for different confounding scenarios.

Although non-parametric and varying coefficient approaches [[Hastie and Tibshirani, 1993](#)] for ER estimation could, in theory, allow for differential confounding across different exposure levels, none of the existing methods for ER estimation explicitly accommodates local confounding, nor provides guidance for which covariates are confounders of the effect of interest at different levels of the exposure. Furthermore, the use of non-parametric methods to estimate a generalized propensity score or model the outcome of interest could prove unfruitful in situations where most of the available data are over a specific range of the exposure variable, the number of potential confounders is large, and interest lies in the estimation of causal effects for change in the exposure in the tails of the exposure distribution. In such situations, LERCA provides a way to model the outcome acknowledging that the exposure-response relationship might be confounded by different covariates at different exposure levels. Lastly, it is worth noting that LERCA shall not be seen as a direct competitor to the approach by [Kennedy et al. \[2017\]](#). In fact, since the Super Learner algorithm combines different approaches for modeling the outcome, LERCA could be incorporated in the algorithm as an approach that allows for the presence of local confounding.

Local confounding in the estimation of an exposure-response function does not pertain solely in the estimation of the health effects of air pollution. In fact, the methodology presented in this paper provides a data driven approach which is applicable to the majority of regulatory settings regarding safety of potential harmful substances, and can be routinely used to assess health effects of low level exposures. Such applications include the effects of lead [[Chiodo et al., 2004](#), [Jusko et al., 2008](#)], environmental contaminants [[Van Der Oost et al., 2003](#)], radiation [[National Research Council, 2006](#),

Fazel et al., 2009], and pesticides [Mackenzie Ross et al., 2010, Androutsopoulos et al., 2012].

## APPENDIX A. DATA DETAILS

We constructed counts corresponding to the cardiovascular-specific (CVD) number of hospitalizations for Medicare enrollees aged at least 65 years during 2013 for a total of 35,373 zip codes across the continental US. Hospitalization rates were based on the total number of personal years for Medicare enrollees for a zip code on a given year. CVD hospitalizations were considered on the basis of primary diagnosis according to International Classification of Diseases, Ninth Revision (ICD-9) codes (ICD-9 390 to 459). The analysis was restricted to the continental US leading to 34,897 zip codes with hospitalization information.

Population demographic information was acquired using the 2000 Census with information on over 400 variables, although a lot of them are highly correlated. We further used linearly extrapolated Census variables for 2013. Census information is provided at a ZCTA level, and we use a crosswalk to map ZCTA to zip code. Weather information including temperature, relative humidity and dew point is acquired from the NOAA-ASOS website, and is linked to zip codes within 150 kilometers.

Lastly, zip code  $PM_{2.5}$  exposure is assigned using the US EPA monitoring sites. By EPA recom-

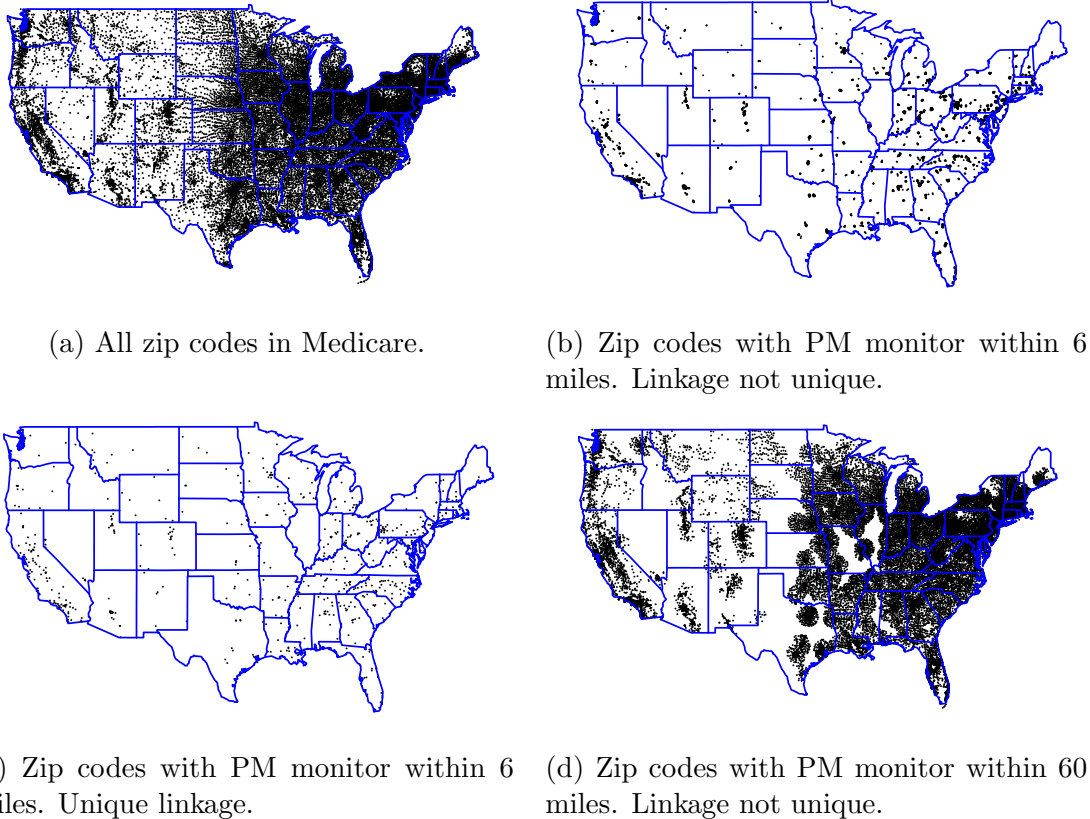


Figure A.1: (a) All zip codes with available Medicare information. (b) Zip codes with available exposure information after performing linkage within 6 miles and monitors are allowed to be linked to more than one zip code. (c) Zip codes with available exposure information after performing linkage within 6 miles where each monitor is only linked to up to one zip code. (d) Zip codes with available exposure information after linkage with monitors within 60 miles and every monitor can be linked to more than one zip code.

mendations, monitoring sites with less than 67% of scheduled measurements observed are excluded. For every monitor, the average of the 2011-2012 average annual value of  $PM_{2.5}$  is calculated, and the monitor is linked to *all* zip codes with centroids within 6 miles. Then, the zip code exposure is set equal to the average over all linked monitors. Since monitoring sites are preferentially located near populated areas or points of interest, many zip codes in remote areas are not linked to any monitor and are therefore dropped from the final data set.

Figure A.1 shows maps of zip code centroids before linkage to EPA monitoring sites, as well as maintained zip code centroids after 3 different linkage procedures corresponding to different specifications of the linkage distance, as well as whether a monitor can be linked to more than one zip code. We visualize how linkage can affect the final data set:

- **Distance:** As the distance of allowed linked zip codes and monitors increases, we expect that more zip codes will be linked to at least one monitor. However, the assigned values of  $PM_{2.5}$  will be more uncertain in areas where monitors are located at long distances.
- **Number of links:** Allowing a monitor to be linked to multiple zip codes increases the number of zip codes with  $PM_{2.5}$  information. However, this can lead to adjacent zip codes with very similar or identical  $PM_{2.5}$  measurements.

Table A.1: Available demographic and weather information

Source	Name	Description	Mean	SD
2000 Census	% White	Percentage of White Population	0.71	0.25
	% Hisp	Percentage of Hispanic Population	0.12	0.18
	% HS	Percentage of population that attended high school	0.27	0.10
	% Poor	Percentage of impoverished population	0.14	0.11
	% Female	Percentage of female population	0.51	0.04
	% Moved in 5	Percentage of population that has lived in the area for less than 5 years	0.50	0.12
	Avg Commute	Mean Travel Time to Work	24.22	5.92
	Population/SQM	Population per square mile (logarithm)	7.53	1.52
	Total Population	Total population (logarithm)	9.71	1.12
	Low Occupied	Indicator. “=1” if the percent of occupied population is at most 90%.	0.211	0.408
	High Occupied	Indicator. “=1” if the percent of occupied population is over 95%.	0.416	0.493
	Low Hispanic	Indicator. “=1” if the percent of Hispanic population is at most 0.02%	0.317	0.465
	High Hispanic	Indicator. “=1” if the percent of Hispanic population is over 20%	0.197	0.398
	Census Extrapolation	% Below HS	Population percent with less than high school education (above age of 65)	23.24
% Own Households		Percentage of occupied housing units in 2013	0.58	0.2
Low Poverty		Indicator. “=1” if the percent of the population below the poverty line in 2013 is at most 5%	0.196	0.397
High Poverty		Indicator. “=1” if the percent of the population below the poverty line in 2013 is over 15%	0.244	0.429
Census combination <sup>1</sup>	House Value	Median value of owner occupied housing (USD) (logarithm)	12.65	0.63

<sup>1</sup>The 2000 Census is combined with the 2013 extrapolated values of the same variable by taking the mean of the variable across the two years.

	Household Income	Median household income (USD) (logarithm)	11.40	0.42
BRFSS	BMI	Average BMI in 2013	27.65	1.32
	Smoking Rate	Ever smoke rate (2013)	0.45	0.06
Weather	Avg Temp	Average temperature (F)	55.35	7.47
	Avg Dew Point	Average Dew Point (F)	44.09	7.50
	Avg Humidity	Average Relative Humidity (%)	70.41	8.34
Medicare	Avg Age	Average Medicare Age	74.89	1.66
	Female Rate	Percentage of Female Beneficiaries	0.55	0.06
	Dual Rate	Percentage of Dual Eligible Beneficiaries	0.22	0.15

## APPENDIX B. PRIOR SPECIFICATIONS FOR REGRESSION PARAMETERS AND EXPERIMENT CONFIGURATION

**B.1 Regression coefficients and residual variance** Prior independences of all parameters are expressed in the following representation

$$\begin{aligned}
& p(\underline{\alpha}^X, \underline{\alpha}^Y, \underline{\delta}^X, \beta_k, \underline{\delta}^Y, \underline{\sigma}_X^2, \underline{\sigma}_Y^2) \\
&= p(\delta_{10}^Y) \prod_{k=1}^{K+1} \left\{ \left[ \prod_{j=1}^p p(\alpha_{kj}^X, \alpha_{kj}^Y) p(\delta_{kj}^X | \alpha_{kj}^X) p(\delta_{kj}^Y | \alpha_{kj}^Y) \right] p(\delta_{k0}^X) p(\beta_k) p(\sigma_{k,X}^2) p(\sigma_{k,Y}^2) \right\}, \quad (\text{B.1})
\end{aligned}$$

for vectors  $\underline{\delta}^Y$  satisfying the recursive prior. We assume non-informative normal priors on  $\beta_k$ ,  $k = 1, 2, \dots, K + 1$ , and  $\delta_{10}^Y$ . The prior distribution on the regression coefficients for the covariates is a mixture of non-informative normal distribution and point-mass at 0. Non-informative inverse gamma prior distributions are assumed on  $\sigma_{k,X}^2, \sigma_{k,Y}^2$ . Specifically

- $\beta_k \sim N(\mu_0, \sigma_0^2)$ ,  $\delta_{10} \sim N(\mu_0, \sigma_0^2)$ .
- $\delta_{kj}^X | \alpha_{kj}^X \sim \alpha_{kj}^X N(\mu_0, \sigma_0^2) + (1 - \alpha_{kj}^X) \mathbb{1}_0(\delta_{kj}^X)$ , where  $\mathbb{1}_0(\delta_{kj}^X)$  is a point-mass distribution at 0. Similarly for  $\delta_{kj}^Y | \alpha_{kj}^Y$ .
- $\sigma_{k,X}^2 \sim IG(a_0, b_0)$ , and similarly for  $\sigma_{k,Y}^2$ .

The hyper-parameters  $\mu_0, \sigma_0^2, a_0, b_0$  can be chosen differently for different variables.

**B.2 Experiment configuration** The prior on the points  $\mathbf{s} = (s_1, s_2, \dots, s_K)$  defining the experiment configuration is set as the even ordered statistics of  $(2K + 1)$  samples from a uniform distribution over the observed exposure range. Compared to a uniform prior distribution on  $\mathbf{s}$ , this choice of a prior discourages the existence of points  $s_i, s_j$  in the experiment configuration that are very close to each other.

Let  $K$  and the exposure range  $(s_0, s_{K+1})$  be fixed. Let  $Z_i \sim U(s_0, s_{K+1})$ ,  $i = 1, 2, \dots, 2K + 1$  and denote the even ordered statistics as  $W_j = Z_{(2j)}$ ,  $j = 1, 2, \dots, K$ . Then,

$$\begin{aligned}
f_{W_1, W_2, \dots, W_K}(w_1, w_2, \dots, w_K) &= \\
& f_{W_1}(w_1) f_{W_2|W_1}(w_2|w_1) \dots f_{W_K|W_1, W_2, \dots, W_{K-1}}(w_K|w_1, w_2, \dots, w_{K-1})
\end{aligned}$$

Since  $W_1$  is th  $2^{\text{nd}}$  order statistic of  $2K + 1$  samples from  $U(s_0, s_{K+1})$ , we know that

$$f_{W_1}(w_1) = \frac{(2K + 1)!}{(2K - 1)!} \frac{1}{s_{K+1} - s_0} \frac{w_1 - s_0}{s_{K+1} - s_0} \left( 1 - \frac{w_1 - s_0}{s_{K+1} - s_0} \right)^{2K-1}$$



$$= \frac{(2K+1)!}{(2K-1)!} (s_{K+1} - s_0)^{-(2K+1)} (w_1 - s_0)(s_{K+1} - w_1)^{2K-1}$$

Given  $W_1 = w_1$ ,  $W_2$  acts like the second order statistic of  $2K - 1$  uniform samples from a uniform distribution over  $(w_1, s_{K+1})$ . Therefore, we similarly get that

$$f_{W_2|W_1}(w_2|w_1) = \frac{(2K-1)!}{(2K-3)!} (s_{K+1} - w_1)^{-(2K-1)} (w_2 - w_1)(s_{K+1} - w_2)^{2K-3}.$$

Iteratively, we have that

$$f_{W_1, W_2, \dots, W_K}(w_1, w_2, \dots, w_K) = (2K+1)! (s_{K+1} - s_0)^{-(2K+1)} (w_1 - s_0)(w_2 - w_1) \dots (w_K - w_{K-1})(s_{K+1} - w_K)$$

Therefore, the prior distribution on  $\mathbf{s}$  with minimum distance of consecutive points  $s_k, s_{k+1}$  being  $d_k$  is defined as

$$f_{\mathbf{s}}(s_1, s_2, \dots, s_K) \propto \prod_{k=0}^K (s_{k+1} - s_k) \mathbb{1}(s_{k+1} - s_k > d_k) \quad (\text{B.2})$$

### APPENDIX C. SAMPLING FROM THE POSTERIOR DISTRIBUTION

The parameters included in the model are:  $\mathbf{s}$  (the exposure values in the experiment configuration),  $\boldsymbol{\alpha}^X, \boldsymbol{\alpha}^Y$  (the vectors of length  $p$  including the covariates' inclusion indicators in the exposure and the outcome model for each experiment),  $\boldsymbol{\beta} = \{\beta_k\}_{k=1}^{K+1}$  (coefficients of exposure in the outcome model),  $\boldsymbol{\delta}^X, \boldsymbol{\delta}^Y$  (intercepts and coefficients of the covariates in the exposure and outcome model of each experiment),  $\boldsymbol{\sigma}_X^2 = \{\sigma_{k,X}^2\}_{k=1}^{K+1}, \boldsymbol{\sigma}_Y^2 = \{\sigma_{k,Y}^2\}_{k=1}^{K+1}$  (residual variance of the exposure and outcome within each experiment).

**C.1 Likelihood factorization** We start by noting that the data likelihood (conditional on all parameters) factorizes to components for different experiments and the exposure and outcome models. If  $\mathbf{Y}, \mathbf{X}$  denote the vectors of outcomes and exposures for all units in the sample, and  $\mathbf{Y}^k, \mathbf{X}^k$  denote the vectors of outcomes and exposures in experiment  $k$ , then

$$P(\mathbf{Y}, \mathbf{X} | \mathbf{s}, \boldsymbol{\alpha}^X, \boldsymbol{\alpha}^Y, \boldsymbol{\delta}^X, \boldsymbol{\delta}^Y, \boldsymbol{\beta}, \boldsymbol{\sigma}_X^2, \boldsymbol{\sigma}_Y^2, \mathbf{C}) = \prod_{k=1}^{K+1} \prod_{i \in g_k} p_k(Y_i | X_i, \boldsymbol{\alpha}_k^Y, \boldsymbol{\delta}_k^Y, \beta_k, \sigma_{k,Y}^2, \mathbf{C}_i) p_k(X_i | \boldsymbol{\alpha}_k^X, \boldsymbol{\delta}_k^X, \sigma_{k,X}^2, \mathbf{C}_i) = \prod_{k=1}^{K+1} [p_k(\mathbf{Y}^k | \mathbf{X}^k, \boldsymbol{\alpha}_k^Y, \boldsymbol{\delta}_k^Y, \beta_k, \sigma_{k,Y}^2, \mathbf{C}^k) p_k(\mathbf{X}^k | \boldsymbol{\alpha}_k^X, \boldsymbol{\delta}_k^X, \sigma_{k,X}^2, \mathbf{C}^k)], \quad (\text{C.1})$$

where we denote  $p_k(\cdot_1 | \cdot_2)$  as the density of  $\cdot_1$  conditional on  $\cdot_2$  in experiment  $k$  and  $\boldsymbol{\delta}_k^Y$  includes the intercept  $\delta_{k0}^Y$ .

Next, we note that if we consider the marginal likelihood integrating out 1) exposure model regression coefficients including the intercept, 2) outcome model covariates' regression coefficients,

and 3) all variance terms, then the likelihood still factorizes in a similar manner. In fact<sup>2</sup>:

$$\begin{aligned}
& P(\mathbf{Y}, \mathbf{X} | \mathbf{s}, \boldsymbol{\alpha}^X, \boldsymbol{\alpha}^Y, \tilde{\boldsymbol{\beta}}, \delta_{10}^Y, \mathbf{C}) \\
&= \int P(\mathbf{Y}, \mathbf{X} | \mathbf{s}, \boldsymbol{\alpha}^X, \boldsymbol{\alpha}^Y, \tilde{\boldsymbol{\delta}}^X, \tilde{\boldsymbol{\delta}}^Y, \tilde{\boldsymbol{\beta}}, \delta_{10}^Y, \boldsymbol{\sigma}_X^2, \boldsymbol{\sigma}_Y^2, \mathbf{C}) \times \\
&\quad p(\tilde{\boldsymbol{\delta}}^X, \tilde{\boldsymbol{\delta}}^Y, \boldsymbol{\sigma}_X^2, \boldsymbol{\sigma}_Y^2 | \mathbf{s}, \boldsymbol{\alpha}^X, \boldsymbol{\alpha}^Y) d(\tilde{\boldsymbol{\delta}}^X, \tilde{\boldsymbol{\delta}}^Y, \boldsymbol{\sigma}_X^2, \boldsymbol{\sigma}_Y^2) \\
&= \prod_{k=1}^{K+1} \int p_k(\mathbf{Y}^k | \mathbf{X}^k, \mathbf{s}, \boldsymbol{\alpha}_k^Y, \tilde{\boldsymbol{\delta}}_k^Y, \tilde{\boldsymbol{\beta}}, \delta_{10}^Y, \sigma_{k,Y}^2, \mathbf{C}^k) p_k(\mathbf{X}^k | \boldsymbol{\alpha}_k^X, \tilde{\boldsymbol{\delta}}_k^X, \sigma_{k,X}^2, \mathbf{C}^k) \times \\
&\quad p(\tilde{\boldsymbol{\delta}}_k^X, \tilde{\boldsymbol{\delta}}_k^Y, \sigma_{k,X}^2, \sigma_{k,Y}^2 | \mathbf{s}, \boldsymbol{\alpha}_k^X, \boldsymbol{\alpha}_k^Y) d(\tilde{\boldsymbol{\delta}}_k^X, \tilde{\boldsymbol{\delta}}_k^Y, \sigma_{k,X}^2, \sigma_{k,Y}^2) \\
&= \prod_{k=1}^{K+1} \int p_k(\mathbf{Y}^k | \mathbf{X}^k, \mathbf{s}, \boldsymbol{\alpha}_k^Y, \tilde{\boldsymbol{\delta}}_k^Y, \tilde{\boldsymbol{\beta}}, \delta_{10}^Y, \sigma_{k,Y}^2, \mathbf{C}^k) p(\tilde{\boldsymbol{\delta}}_k^Y, \sigma_{k,Y}^2 | \mathbf{s}, \boldsymbol{\alpha}_k^Y) d(\tilde{\boldsymbol{\delta}}_k^Y, \sigma_{k,Y}^2) \\
&\quad \int p_k(\mathbf{X}^k | \boldsymbol{\alpha}_k^X, \tilde{\boldsymbol{\delta}}_k^X, \sigma_{k,X}^2) p(\tilde{\boldsymbol{\delta}}_k^X, \sigma_{k,X}^2 | \mathbf{s}, \boldsymbol{\alpha}_k^X) d(\tilde{\boldsymbol{\delta}}_k^X, \sigma_{k,X}^2) \\
&= \prod_{k=1}^{K+1} p_k(\mathbf{Y}^k | \mathbf{X}^k, \mathbf{s}, \boldsymbol{\alpha}_k^Y, \delta_{k0}^Y, \tilde{\boldsymbol{\beta}}, \mathbf{C}^k) p_k(\mathbf{X}^k | \boldsymbol{\alpha}_k^X, \mathbf{C}^k) \tag{C.2}
\end{aligned}$$

where the second equation holds from the factorization of the likelihood (when  $\tilde{\boldsymbol{\delta}}_k^Y$  does not include the intercepts we need to condition on  $\delta_{10}^Y$  and  $\tilde{\boldsymbol{\beta}}$ ) and the assumed prior independences.

## C.2 Sampling all model parameters using MCMC

*C.2.1 Sampling the regression coefficients and residual variance terms* The factorization of the full data likelihood over experiments and exposure/outcome models and the choice of the prior distributions lead to full conditional posterior distributions of coefficients  $\delta_{k0}^X, \delta_{kj}^X, \delta_{kj}^Y$ , and variance terms  $\sigma_{k,X}^2, \sigma_{k,Y}^2$  of known forms. The variance terms and exposure model intercepts have inverse Gamma and normal full conditional posterior distributions accordingly, whereas the distributions of  $\delta_{kj}^X, \delta_{kj}^Y$  are either point mass at 0 or normal, based on whether the corresponding  $\alpha$  is 0 or 1.

We update coefficients  $\delta_{kj}^X$  for which  $\alpha_{kj}^X = 0$  separately from the ones with  $\alpha_{kj}^X = 1$ . Parameters  $\delta_{kj}^X$  for which  $\alpha_{kj}^X = 0$  are set to 0. Let  $j_1, j_2, \dots, j_{N_x}$  be the indices such that  $\alpha_{kj_l} = 1, l = 1, 2, \dots, N_x$ . Then,

$$\begin{aligned}
& (\delta_{k0}^X, \delta_{kj_1}^X, \delta_{kj_2}^X, \dots, \delta_{kj_{N_x}}^X)^T | \text{Data}, \cdot \sim MVN_{N_x+1}(\boldsymbol{\mu}_X, \boldsymbol{\Sigma}_X), \\
& \text{where } \boldsymbol{\Sigma}_X = \left( \frac{1}{\sigma_{k,X}^2} \tilde{\mathbf{V}}^T \tilde{\mathbf{V}} + \frac{1}{\sigma_0^2} I_{N_x+1} \right)^{-1} \text{ and } \boldsymbol{\mu}_X = \boldsymbol{\Sigma}_X \left( \frac{1}{\sigma_{k,X}^2} \tilde{\mathbf{V}}^T \mathbf{X}^k + \frac{1}{\sigma_0^2} \tilde{\boldsymbol{\mu}}_0 \right)
\end{aligned}$$

where  $\tilde{\mathbf{V}} = (\mathbf{1}, \mathbf{C}_{j_1}^k, \mathbf{C}_{j_2}^k, \dots, \mathbf{C}_{j_{N_x}}^k)$  is the design matrix of data in experiment  $k$  based on the included covariates, and  $\tilde{\boldsymbol{\mu}}_0$  is a vector of length  $N_x + 1$  of repeated values  $\mu_0$ . (Update of the coefficients  $\delta_{kj}^Y$  is performed conditional on  $\delta_{k0}^Y, \tilde{\boldsymbol{\beta}}$  and is similar to the updates of the coefficients in the exposure model and therefore omitted.)

<sup>2</sup>In the following,  $\tilde{\boldsymbol{\delta}}^X$  includes the exposure model intercepts, but  $\tilde{\boldsymbol{\delta}}^Y$  includes only the coefficients of the covariates.

The full conditional distribution of the variance term  $\sigma_{k,X}^2$  is also of known form

$$\sigma_{k,X}^2 | \text{Data}, \bullet \sim IG(a_X, b_X),$$

where  $a_X = a_0 + \frac{n_k}{2}$ ,  $b_X = b_0 + \frac{1}{2}(\mathbf{X}^K - \mathbf{V}\boldsymbol{\delta}_k^X)^T(\mathbf{X}^k - \mathbf{V}\boldsymbol{\delta}_k^X)$ ,

where  $n_k$  is the number of observations in experiment  $k$ , and  $\mathbf{V} = (\mathbf{1}, \mathbf{C}^k)$ . (The full conditional posterior distribution of  $\sigma_{k,Y}^2$  is very similar and is therefore omitted.)

It is worth noting that centering the covariates  $C_j$  allows the outcome model intercepts  $\delta_{k0}$  to depend solely on  $\delta_{10}$ ,  $\beta_k$  and  $\mathbf{s}$ , and not on  $\delta_{kj}^Y$ . This simplifies the form of the full conditional distribution for many coefficients. Since  $\delta_{k0}^Y$ ,  $k \geq 2$  is a deterministic function of  $\delta_{10}$ ,  $\beta_1, \beta_2, \dots, \beta_{k-1}$ , and the points  $s_0, s_1, \dots, s_k$ , the full conditional posterior distribution of  $\delta_{10}$  depends on data across all experiments, and that of  $\beta_k$  on data from experiment  $k$  and onwards. Since the data likelihood in all experiments is normal and we have assumed normal prior distributions, the full conditional posterior distributions are also normal. After each update, intercepts  $\delta_{k0}^Y$ ,  $k \geq 2$  need to be updated from (5) to ensure ER continuity.

The parameter  $\delta_{10}^Y$  is included in the mean structure of the outcome model for all experiments. Its full conditional posterior distribution is  $\delta_{10}^Y | \text{Data}, \bullet \sim N(\mu, \sigma^2)$  where

$$\sigma^2 = \left( \frac{1}{\sigma_0^2} + \sum_{k=1}^{K+1} \frac{n_k}{\sigma_{k,Y}^2} \right)^{-1}$$

and

$$\mu = \sigma^2 \left[ \frac{\mu_0}{\sigma_0^2} + \sum_{k=1}^{K+1} \frac{1}{\sigma_{k,Y}^2} \sum_{i \in g_k} \left( y_i - \sum_{l=1}^{k-1} \beta_l (s_l - s_{l-1}) - \beta_k (x_i - s_{k-1}) - \sum_{j=1}^p \delta_{kj}^Y C_{ij} \right) \right],$$

where  $\sum_a^b = 0$  if  $b < a$ . Similarly, the full conditional posterior distribution of  $\beta_k$  uses data from experiments  $k, k+1, \dots, K+1$ , and is  $\beta_k | \text{Data}, \bullet \sim N(\mu, \sigma^2)$  where

$$\sigma^2 = \left( \frac{1}{\sigma_0^2} + \frac{1}{\sigma_{k,Y}^2} \sum_{i \in g_k} (x_i - s_{k-1})^2 + (s_k - s_{k-1})^2 \sum_{l=k+1}^{K+1} \frac{n_l}{\sigma_{l,Y}^2} \right)^{-1}$$

and

$$\mu = \sigma^2 \left( \frac{\mu_0}{\sigma_0^2} + \frac{1}{\sigma_{k,Y}^2} \sum_{i \in g_k} (x_i - s_{k-1})(y_i - \delta_{k0}^Y - \sum_j \delta_{kj}^Y C_{ij}) + \sum_{l=1}^{K+1} \frac{1}{\sigma_{l,Y}^2} \sum_{i \in g_l} (s_k - s_{k-1})(y_i - \delta_{k0}^Y - \sum_{e=k+1}^{l-1} \beta_e (s_e - s_{e-1}) - \beta_l (x_i - s_{l-1}) - \sum_j \delta_{lj}^Y C_{ij}) \right)$$

*C.2.2 Sampling the experiment configuration and inclusion indicators* The experiment configuration and inclusion indicators can be updated separately, or simultaneously. We first describe the separate update of  $\mathbf{s}$  and  $(\boldsymbol{\alpha}^X, \boldsymbol{\alpha}^Y)$ , and afterwards we will discuss why occasional simultaneous sampling was deemed necessary. One of the three moves (separate, jump over, jump within) depicted in Figure C.1 is performed at every iteration with probability 0.8, 0.1, and 0.1 accordingly.

**(separate)** The experiment configuration and inclusion indicators are updated separately and conditionally on each other. For the update of the experiment configuration  $\mathbf{s}$ , a Metropolis-Hastings step is used [Metropolis et al., 1953, Hastings, 1970] based on the full conditional likelihood (C.1).  $k$  is chosen uniformly over  $\{1, 2, \dots, K\}$  and  $s^* \sim U(s_{k-1}, s_{k+1})$  is drawn as shown in Figure C.1(b). Alternatively,  $s^*$  could be sampled from a truncated normal distribution centered at  $s_k$ . If  $s^*$  violates  $s_{k+1} - s^* \geq d_k$  or  $s^* - s_{k-1} \geq d_{k-1}$ , the move is automatically rejected.

Otherwise, the move  $\mathbf{s} \rightarrow \mathbf{s}^* = (s_1, s_2, \dots, s_{k-1}, s^*, s_{k+1}, \dots, s_K)$  is proposed with all other parameters (excluding  $\boldsymbol{\beta}$ ) fixed to their current values. Proposing new values of  $\boldsymbol{\beta}$  is necessary to ensure that the ER  $\tilde{\omega}$  is continuous at the proposed state. All coefficients but  $\beta_k, \tilde{\beta}_{k+1}$  are fixed to their current values, and new values for  $\beta_k, \beta_{k+1}$  are proposed such that the intercepts of the adjacent experiments are also fixed. If  $s^* < s_k$ , the proposed value  $\beta_{k+1}^*$  is sampled from a uniform distribution between the values  $\beta_{k+1}$  (current state) and

$$\tilde{\beta}_{k+1} = (s_{k+1} - s^*)^{-1}(\delta_{(k+2)0}^Y - \delta_{k0}^Y - \beta_k(s^* - s_{k-1})),$$

where  $\tilde{\beta}_{k+1}$  is the slope that would connect the value of the ER at point  $s_{k+1}$  with the value of the ER at point  $s^*$  at the current state. Figure C.2 shows the limits of the proposed ER. Based on the sampled value for  $\beta_{k+1}^*$ , the proposed value for  $\beta_k$  is

$$\beta_k^* = (s^* - s_{k-1})^{-1}(\delta_{(k+2)0}^Y - \delta_{k0}^Y - \beta_{k+1}^*(s_{k+1} - s^*)).$$

Similarly for  $s^* > s_k$  by sampling  $\beta_k^*$  from a uniform that has similar properties.

Since the likelihood factorizes as shown in (C.1) the likelihood ratio of the Metropolis-Hastings acceptance probability includes terms only for experiments  $k, k+1$ . The prior ratio includes terms for the experiment configuration distribution in (B.2), and the prior for  $\beta_k, \beta_{k+1}$ . If a uniform distribution is used to sample  $s^*$ , the proposal for the cutoffs is symmetric, and the proposal ratio corresponds to the proposal ratio for coefficients  $\beta_k, \beta_{k+1}$ . This is equal to  $|\beta_{k+1} - \tilde{\beta}_{k+1}|/|\beta_k^* - \tilde{\beta}_k^*|$ , where  $\beta_k^*$  is the proposed value and  $\tilde{\beta}_k^*$  is the one boundary of the proposal distribution for  $\beta_k$  in the reverse move.

After we accept or reject the move  $\mathbf{s} \rightarrow \mathbf{s}^*$ , we update the inclusion indicators based on their full

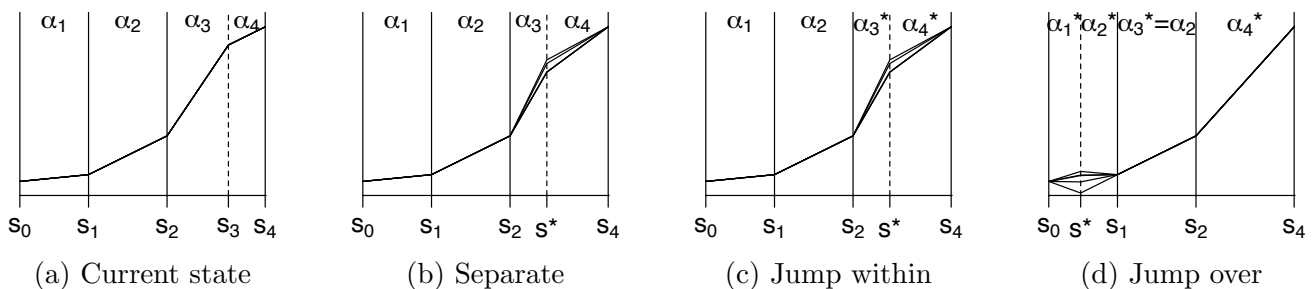


Figure C.1: Proposed state for the separate, jump within and jump over moves are depicted schematically for a hypothetical experiment configuration with  $K = 3$ . In all proposed states, new slopes are proposed to ensure continuity of the ER. (a) The current state of the MCMC.  $s_3$  is chosen to be updated. (b) A new point  $s^*$  is proposed within  $(s_2, s_4)$  with the corresponding  $\alpha$  parameters constant. (c) Simultaneous move of the experiment configuration and the corresponding  $\alpha$ 's within  $(s_2, s_4)$ . (d) The proposed point  $s^*$  is located outside the interval  $(s_2, s_4)$  and new  $\alpha$ 's are proposed for the experiment that was split  $(s_0, s_1)$ , and the experiments that were combined  $(s_2, s_4)$ .

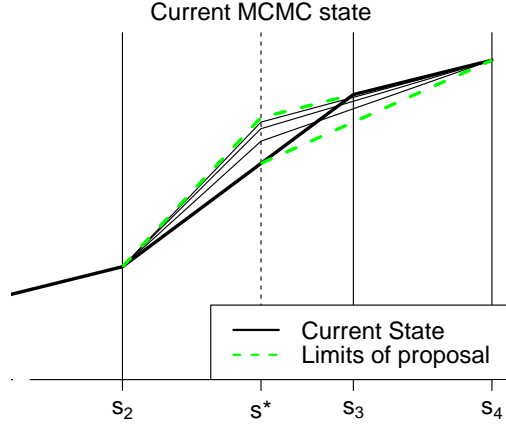


Figure C.2: Values of  $\beta_k, \beta_{k+1}$  for the separate move are proposed such that the estimated ER are within the limits shown in dashed green lines. The black solid line correspond to the current state of the ER.

conditional. Let  $A^*$  be all parameters but  $\alpha_{kj}^X, \alpha_{kj}^Y$  and  $\delta_{kj}^Y$ . For  $\alpha \in \{0, 1\}$

$$\begin{aligned}
p(\alpha_{kj}^Y = \alpha | \text{Data}, A^*, \alpha_{kj}^X) &= \frac{p(\delta_{kj}^Y = 0, \alpha_{kj}^Y = \alpha | \text{Data}, A^*, \alpha_{kj}^X)}{p(\delta_{kj}^Y = 0 | \alpha_{kj}^Y = \alpha, \text{Data}, A^*, \alpha_{kj}^X)} \\
&= \frac{p(\text{Data}, A^* | \delta_{kj}^Y = 0, \alpha_{kj}^Y = \alpha, \alpha_{kj}^X) p(\delta_{kj}^Y = 0, \alpha_{kj}^Y = \alpha | \alpha_{kj}^X)}{p(\text{Data}, A^* | \alpha_{kj}^X) p(\delta_{kj}^Y = 0 | \alpha_{kj}^Y = \alpha, \text{Data}, A^*, \alpha_{kj}^X)} \\
&\propto \frac{p(\delta_{kj}^Y = 0 | \alpha_{kj}^Y = \alpha, \alpha_{kj}^X) p(\alpha_{kj}^Y = \alpha | \alpha_{kj}^X)}{p(\delta_{kj}^Y = 0 | \alpha_{kj}^Y = \alpha, \text{Data}, A^*, \alpha_{kj}^X)} \\
&= \frac{p(\delta_{kj}^Y = 0 | \alpha_{kj}^Y = \alpha) p(\alpha_{kj}^Y = \alpha | \alpha_{kj}^X)}{p(\delta_{kj}^Y = 0 | \alpha_{kj}^Y = \alpha, \text{Data}, A^*)}, \quad \alpha \in \{0, 1\}, \tag{C.3}
\end{aligned}$$

where the numerator consists of the product of two prior probabilities, and the denominator consists of the posterior probability that  $\delta_{kj}^Y = 0$ . This has been seen previously in a different context [Antonelli et al., 2017a], and consists a computational improvement over previous implementations of this prior distribution that utilized the MC<sup>3</sup> algorithm [Madigan et al., 1995, Wang et al., 2012].

However, sampling the inclusion indicators and experiment configuration separately can lead to slow convergence. For example, consider our simulation scenario where the true experiment configuration is (2, 4, 7), and starting values randomly set to (0.5, 2, 7). Based on the separate move, point  $s_1$  is always proposed to be updated between  $s_0, s_2 = 2$ , which can lead to slow mixing. The jump over and jump within moves are meant to alleviate such issues.

In order to avoid the need of proposing values for the covariates' coefficients and variance terms in the update of the experiment configuration through a simultaneous move, these parameters are integrated out from the data likelihood. Integrating all other parameters out allows us to perform sampling of the experiment configuration without heavy fine tuning of proposal distributions. In both situations, sampling of  $\mathbf{s}, \underline{\alpha}^X, \underline{\alpha}^Y, \underline{\beta}$  is performed using the marginalized likelihood (C.2):

$$p(\mathbf{s}, \underline{\alpha}^X, \underline{\alpha}^Y, \underline{\beta} | \text{Data}, \delta_{10}^Y) \propto p(\mathbf{Y}, \mathbf{X} | \mathbf{s}, \underline{\alpha}^X, \underline{\alpha}^Y, \underline{\beta}, \delta_{10}^Y, \mathbf{C}) p(\mathbf{s}) p(\underline{\alpha}^X, \underline{\alpha}^Y) p(\underline{\beta}).$$

Note that all likelihoods in (C.2) are marginal densities of linear regression models over the regression coefficients and variance terms with Normal-Inverse Gamma priors. Raftery et al. [1997] provided closed form calculations of this marginal likelihood. However, this calculation requires the inversion of a matrix with dimension equal to the number of observations, and is computationally intensive. Since the marginal likelihood is only used in the calculation of Bayes factors, we approximate the Bayes factors when necessary using the BIC [Raftery, 1995].

**(jump over)** This move is designed to alleviate the MCMC issue described above by proposing a simultaneous move of  $(\mathbf{s}, \underline{\alpha}^X, \underline{\alpha}^Y, \underline{\beta})$ .  $k \in \{1, 2, \dots, K\}$  is again chosen uniformly, but now a new location of the experiment configuration  $s^*$  is generated uniformly over  $(s_0, s_{K+1}) \setminus [s_{k-1}, s_{k+1}]$ . The move  $\mathbf{s} \rightarrow \mathbf{s}^* = (s_1, s_2, \dots, s_{k-1}, s_{k+1}, \dots, s_{j-1}, s^*, s_j, \dots, s_K)$  proposes a combination of experiments  $k, k+1$  and a split in some randomly chosen experiment  $j$ . For example, in Figure C.1(d), the proposed move splits the first experiment  $(s_0, s_1)$  in two  $(s_0, s^*), (s^*, s_1)$ , and combines the experiments  $(s_2, s_3), (s_3, s_4)$ .

The inclusion indicators of the unchanged experiments remain to their current values, but new values need to be proposed for the combined or split experiments. The assignment of proposed values for the inclusion indicators is probabilistic based on their current values, encouraging the inclusion of a covariate in the proposed state to resemble that of the current state. For example, in Figure C.1(d)  $\alpha_1^*, \alpha_2^*$  should resemble  $\alpha_1$ , and similarly for  $\alpha_4^*$ . In this example, covariates are included in experiment 4 with very low, mediocre and very high probability if none, one or both of the original experiments include it. The values chosen for these probabilities were  $(0.01, 0.5, 0.99)$  accordingly. Similarly, a variable is proposed to be included in the model of experiments 1 and 2 with low and high probability if the variable was included in the initial model or not. The values chosen were  $(0.2, 0.95)$ .

Values for  $\underline{\beta}$  are proposed to ensure that the proposed state corresponds to a continuous ER. Unchanged experiments remain the same. Experiments are combined by connecting the edges of the two linear segments, and values of the split experiments are proposed using a normal perturbation of the current value with variance  $\sigma_{tune}^2$ . Figure C.1(d) shows proposed states of the ER.

The move is accepted or rejected with probability equal to the product of the following:

1. The likelihood ratio for split and combined experiments approximated using the BIC for the exposure model and the outcome model (regressing  $\mathbf{Y}^k - (\mathbb{1}, \mathbf{X}^k - s_{k-1}\mathbb{1})(\delta_{k0}^Y, \beta_k)^T$  on  $\mathbf{C}^k$  without an intercept).
2. The prior ratio for the experiment configuration (B.2), the inclusion indicators (4), and the coefficients  $\beta_k$  for the combined and split experiments.
3. The proposal ratio for  $\mathbf{s}$ ,  $\beta_k$  and  $(\underline{\alpha}^X, \underline{\alpha}^Y)$

$$\frac{(s_{K+1} - s_0) - (s_j - s_{j-1})}{(s_{K+1} - s_0) - (s_{k+1} - s_{k-1})} \exp \left\{ \frac{u^2 - u^{*2}}{2\sigma_{tune}^2} \right\} \prod_{\substack{l \in \{0,1,2\} \\ m \in \{0,1\}}} (p_{lm}^c)^{n_{ml}^s - n_{lm}^c} \prod_{\substack{l \in \{0,1\} \\ m \in \{0,1,2\}}} (p_{lm}^s)^{n_{ml}^c - n_{lm}^s},$$

where  $p_{lm}^c$  is the probability of proposing  $\alpha = m \in \{0, 1\}$  in the combined experiment when  $l \in \{0, 1, 2\}$  of the two initial experiments had  $\alpha = 1$ ,  $p_{lm}^s$  is the probability of proposing  $\alpha = 1$  in  $m \in \{0, 1, 2\}$  of the two experiments when the initial experiment chosen to be split had  $\alpha = l \in \{0, 1\}$ , and  $n_{lm}^c, n_{lm}^s$  is the number of times that each event occurred when moving from the current to the proposed state. Lastly,  $u$  is the difference of the slope for the experiment that was split from the slope of the first split experiment in the proposed state, and  $u^*$  is the difference

of the slope in the first of the experiment that is combined from the slope of the combined experiment in the proposed state.

**(jump within)** This move is similar to the “jump over” but maintaining the ordering of the locations in  $\mathbf{s}$ .  $k \in \{1, 2, \dots, K\}$  is again chosen uniformly, and a new value  $s^*$  is proposed within the interval  $(s_{k-1}, s_{k+1})$ . New values for the coefficients  $\beta_k, \beta_{k+1}$  are proposed as in the separate move. New values of the inclusion indicators are also proposed for the experiments  $k, k + 1$ . In fact,  $C_j$  is proposed to be included in the outcome model of an experiment with high probability if both current models include it, mediocre probability if only one of the models include it, and low probability if none of the models include it. Similarly for the inclusion indicators of the exposure model. The acceptance probability of this move is similar to the one described above, and is omitted here. Figure C.1(c) depicts random draws for proposed ER states.

**C.3 MCMC convergence** Due to the update of the experiment configuration, commonly used convergence diagnostics such as trace plots are not appropriate since parameters (e.g.,  $\beta_k$ ) may correspond to a different range of exposure values at different iterations. Therefore, convergence must be examined in the context of quantities that are detached from the experiment configuration.

One quantity that we use for convergence inspection is the mean exposure response curve calculated over a set of exposure values within the exposure range. Such a set might be an equally spaced grid of points over the interval  $(s_0, s_{K+1})$ , denoted by  $\mathcal{G}$ . For each value  $x \in \mathcal{G}$  and MCMC iteration  $t$ , identify the experiment  $k = k_t(x)$  that  $x$  belongs to. Then, for observation  $i$  calculate the expected response at value  $x$ , by defining  $\tilde{w}_i(x) = (1, x, C_{i1}, \dots, C_{ip})^T$  and calculating  $\hat{Y}_{it}(x) = \tilde{w}_i(x)^T \gamma_{kt}$  where  $\gamma_{kt}$  is the posterior sample of  $(\delta_{k0}^Y, \beta_k, \delta_{k1}^Y, \dots, \delta_{kp}^Y)^T$  in iteration  $t$ . Finally, the  $t$ -posterior sample of the mean response at point  $x \in \mathcal{G}$  is the average of the expected responses over the individuals in the sample  $\hat{Y}_t(x) = \frac{1}{n} \sum_{i=1}^n \hat{Y}_{it}(x)$ .

Convergence could be examined by visual inspection of trace plots of  $\hat{Y}(x)$  for all  $x \in \mathcal{G}$ . Based on multiple chains of the MCMC, we calculate the potential scale reduction factor (PSR) for the mean response at every point  $x \in \mathcal{G}$  [Gelman and Rubin, 1992]. We consider that the MCMC has converged if  $|\text{PSR} - 1| < c$  for all  $x \in \mathcal{G}$ . An alternative quantity based on which MCMC convergence can be examined is  $\hat{\Delta}(x) = \beta_{k_t(x)}$ .

#### APPENDIX D. SIMULATING DATA WITH DIFFERENTIAL CONFOUNDING AT DIFFERENT EXPOSURE LEVELS

In simulation studies, data are most often simulated in the following order: covariates  $C_1, C_2, \dots, C_p$ , exposure  $X$  given a subset of  $C_1, C_2, \dots, C_p$ , and outcome  $Y$  given  $X$  and a potentially different subset of  $C_1, C_2, \dots, C_p$ . Data with differential confounding at different exposure levels could imply, in its most generality, that the exposure  $X$  is generated with different predicting variables at different exposure levels. Generating data with such structure is complicated since the actual  $X$  values define the exposure level that an observation belongs to, and the exposure level in which an observation belongs to defines the set of predictors. For that reason, instead of following the  $\mathbf{C}, X|\mathbf{C}$  approach to data simulation, we generate the exposure values  $X$  first, and  $\mathbf{C}$  is generated conditional on  $X$ , ensuring that the target experiment-specific mean and variance of  $X, \mathbf{C}$ , and correlation of all variables remain the same, as if the data were generated with the typical  $\mathbf{C}, X|\mathbf{C}$  order. Generating the outcome with different predictors at different exposure levels is straightforward by including terms of the form  $\delta_j^* C_j I(X \geq s_k)$ , or by using a separate outcome model within each experiment. In all situations, one should ensure that data are generated in such a way that the true ER is continuous.

**D.1 The “target” data generating mechanism** Given  $K, \mathbf{s}$ , we would like the exposure  $X$  to be generated such as  $E(X)$  and  $Var(X)$  are controllable quantities, since they are closely related to the exposure range of each experiment, and we would like to ensure that simulation results are not driven by the inherit variability in  $X$ . Furthermore, we would like to ensure that  $Var(C_j)$  is approximately the same across experiments and across covariates, such that the the magnitude of  $\delta_{kj}^Y$  has similar interpretation in terms of correlation.

As discussed above, data  $(X, \mathbf{C})$  are usually generated in the order  $\mathbf{C}$  followed by  $X|\mathbf{C}$ , using a model for which  $E(X|\mathbf{C}) = \delta_0 + \sum_{j=1}^p \delta_j C_j$ . Instead of setting target values for  $\delta_j$ , we set target correlations  $Cor(X, C_j)$  and calculate the  $\delta_j$ 's that correspond to these correlations. (The reverse is also possible but requires ensuring that that  $Var(X) \geq \sum_{j=1}^p \delta_j^2 Var(C_j)$ .) We require that  $E(C_j|X = x)$  is continuous in  $x$  to ensure that the joint distribution  $(X, C_j)$  is realistic, and does not have “jumps” at the points of the experiment configuration.

Based on the above, the following represent target (controllable) quantities of our data generation:

- $Var(X), E(X)$  are fixed,
- Within each experiment  $C_j$  are independent random variables with known variance,
- The function  $E(C_j|X = x)$  is continuous in  $x$ ,
- $Cor(C_j, X)$  are fixed and  $\delta_j$  can be calculated, using  $Cor(X, C_j) = \delta_j \sqrt{\frac{Var(C_j)}{Var(X)}}$ .

Ensuring that  $E(C_j|X = x)$  is continuous in  $x$  across experiments is performed in the following way: Given  $Var(X)$ , a model for  $\mathbf{C}|X$  that gives rise to data with the target  $Var(C_j), Cor(X, C_j)$  is considered. The variance-covariance targets do not impose any restrictions on the model intercept. For the first experiment, the intercept can be chosen arbitrarily, and for the subsequent experiments intercepts are chosen to ensure that  $\lim_{t \rightarrow x^-} E(C_j|X = t) = \lim_{t \rightarrow x^+} E(C_j|X = t)$  at all points  $x$ .

**D.2 Generating the data set maintaining target quantities** As discussed in Appendix D.1,  $Cor(X, C_j), Var(C_j)$ , and  $Var(X)$  are considered known, from which we can derive  $Cov(X, C_j)$ . We generate data with the following order:

1.  $X$  is generated from a distribution with mean  $E(X)$ , and variance  $Var(X)$ . In our simulations  $X$  is uniform over the exposure range.
2. Taking advantage of the laws of the multivariate normal distribution we generate

$$\begin{aligned} \mathbf{C}|X &\sim MVN_p(\bar{\mu}, \bar{\Sigma}), \text{ where} \\ \bar{\mu} &= E(\mathbf{C}) + \frac{Cov(\mathbf{C}, X)}{Var(X)}(X - EX), \text{ and} \\ \bar{\Sigma} &= V(\mathbf{C}) - \frac{1}{Var(X)}Cov(\mathbf{C}, X)Cov(\mathbf{C}, X)^T, \end{aligned}$$

where  $Cov(\mathbf{C}, X) = (Cov(C_1, X), Cov(C_2, X), \dots, Cov(C_p, X))^T$ , and  $V(\mathbf{C})$  is a diagonal  $p \times p$  matrix with entries  $Var(C_j), j = 1, 2, \dots, p$ .

3. The marginal means of each variable  $C_j$  within each experiment is calculated by ensuring that the function  $E(C_j|X = x)$  which corresponds to the  $j^{th}$  entry of the vector  $\bar{\mu}$  is continuous at the points of experiment change.



4. Covariates  $C_j$  are subtracted their overall mean.

A simple linear regression form is used to generate the outcome within each experiment. In experiment  $k$ , the outcome is generated from  $Y|X, \mathbf{C} \sim N(\xi_{k0} + \xi_{k1}\phi(X) + \sum_{j=1}^p \xi_{k(j+1)}C_j, \sigma_{k,Y}^2)$ , where  $\phi(\cdot)$  is a continuous function, and the residual variance  $\sigma_{k,Y}^2$  is set equal across  $k$ . We ensure that the true ER function  $E(Y|X)$  is continuous in  $X$  by appropriately setting the intercept values  $\xi_{k0}$ . The intercept in experiment 1 is decided, and for each experiment onwards we set  $\xi_{k0}$  such that

$$\lim_{x \rightarrow s_k^-} E[Y|X = x] = \lim_{x \rightarrow s_k^+} E[Y|X = x] \iff \xi_{(k+1)0} = \xi_{k0} + (\xi_{k1} - \xi_{(k+1)1})\phi(s_k).$$

## APPENDIX E. ADDITIONAL SIMULATION RESULTS

**E.1 Simulations in the presence of local confounding** Table E.1 shows the correlation of the covariates with the exposure and the coefficients of the covariates in the outcome model for the data simulating scenario with local confounding: different confounders at different levels of the exposure.

Figure E.1 shows the the root MSE (rMSE) as a function of the exposure value  $x \in (0, 10)$ . LERCA has the lowest rMSE at the low exposure levels followed by GAM. Root MSE across most methods seems to be comparable for the middle exposure values, and GAM performs slightly better than LERCA at high levels.

Table E.1: Correlation between the covariates and exposure, and outcome coefficients in each experiment, for scenarios with local confounding.

	Covariate - Exposure				Covariate - Outcome			
	$x \in g_1$	$x \in g_2$	$x \in g_3$	$x \in g_4$	$x \in g_1$	$x \in g_2$	$x \in g_3$	$x \in g_4$
$C_1$	0.423	0.525	0.402	0	0.641	0	0	0
$C_2$	0.524	0.572	0	0.503	0.962	0.919	0.593	0.651
$C_3$	0.522	0	0.447	0	0.646	0.643	0.616	0.58
$C_4$	0	0.528	0	0	0	0.633	0	0
$C_5$	0	0	0.533	0.539	0	0	0.658	0
$C_6$	0	0	0	0.509	0	0	0	0.52
$C_7$	0	0	0	0	0	0	0	0
$C_8$	0	0	0	0	0	0	0	0

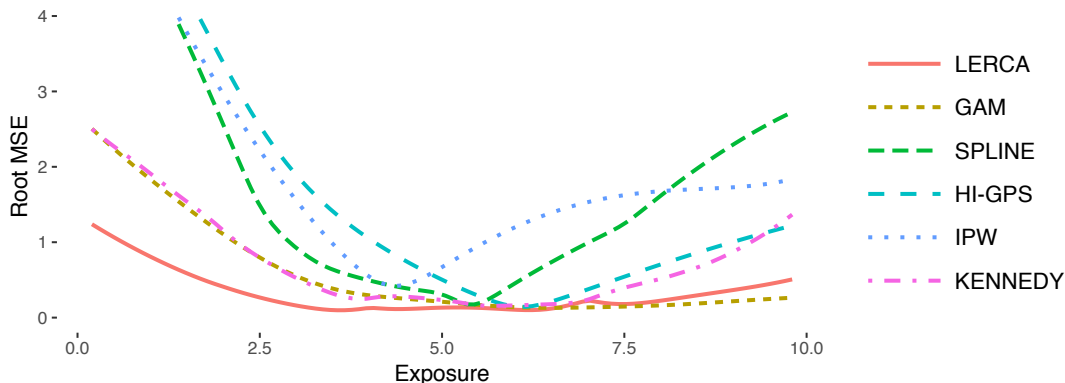


Figure E.1: Mean Root MSE as a function of the exposure  $x \in (0, 10)$ .

**E.2 Simulations in the presence of global confounding** Briefly, data are generated with covariates  $C_1, C_2, C_3$  as predictors of exposure and  $C_2, C_3, C_4$  as predictors of the outcome and the adjusted R-squared of the true exposure and outcome models was 0.73 and 0.94 accordingly. Table E.2 shows the correlation of covariates with the exposure and the outcome model coefficients in the data simulating scenario with global confounding (same confounders with constant confounding strength across exposure levels) and true quadratic ER. Figure E.2 shows the estimated ER for each data set and the average estimated ER based on LERCA and alternative methods. In Figure E.3, the root MSE for all methods is plotted as a function of the exposure  $x \in (0, 10)$ .

Table E.2: Correlation between the covariates and exposure, and outcome coefficients in each experiment, for the scenario with global confounding.

	$C_1$	$C_2$	$C_3$	$C_4$	$C_5$	$C_6$	$C_7$	$C_8$
Exposure	0.423	0.524	0.522	0	0	0	0	0
Outcome	0	0.812	0.93	0.82	0	0	0	0

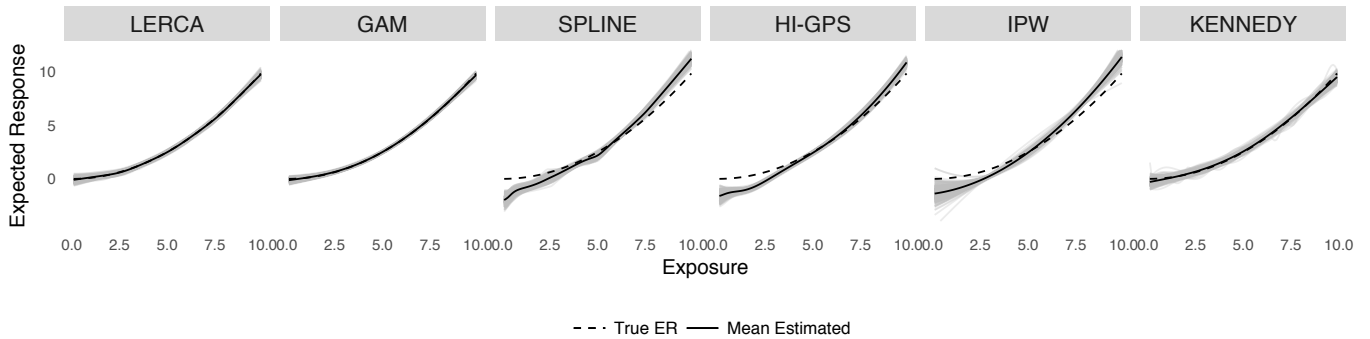


Figure E.2: Simulation results in the presence of global confounding. Grey lines correspond to estimated ER for each simulated data set, solid lines correspond to the mean ER over all simulated data sets, and the dashed line corresponds to the true ER.

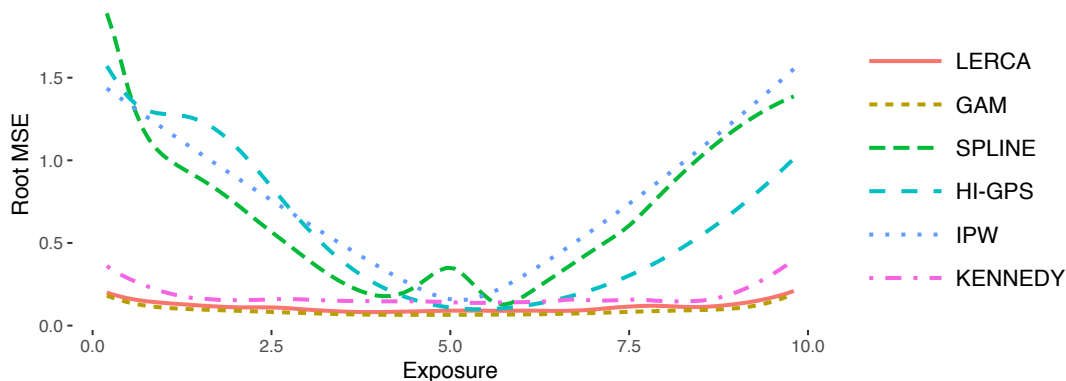


Figure E.3: Root MSE of all methods in the presence of global confounding as a function of the exposure  $x \in (0, 10)$ .

## REFERENCES

- Vasilis P. Androutsopoulos, Antonio F. Hernandez, Jyrki Liesivuori, and Aristidis M. Tsatsakis. A mechanistic overview of health associated effects of low levels of organochlorine and organophosphorous pesticides. *Toxicology*, 307:89–94, 2012.
- Joseph Antonelli, Maitreyi Mazumdar, David Bellinger, David C Christiani, Robert Wright, and Brent A Coull. Bayesian variable selection for multi-dimensional semiparametric regression models. 2017a.
- Joseph Antonelli, Corwin Zigler, and Francesca Dominici. Guided Bayesian imputation to adjust for confounding when combining heterogeneous data sources in comparative effectiveness research. *Biostatistics*, 18(3):553–568, 2017b.
- Joseph Antonelli, Giovanni Parmigiani, and Francesca Dominici. High-dimensional confounding adjustment using continuous spike and slab priors. 2018.
- James Babb, André Rogatko, and Shelemyahu Zacks. Cancer phase I clinical trials: efficient dose escalation with overdose control. *Statistics in Medicine*, 17(10):1103–20, 1998. doi: 10.1002/(SICI)1097-0258(19980530)17:103.0.CO;2-9.
- Michelle L Bell, Roger D Peng, and Francesca Dominici. The exposure-response curve for ozone and risk of mortality and the adequacy of current ozone regulations. *Environmental health perspectives*, 114(4):532–6, apr 2006. ISSN 0091-6765.
- Rebecca E. Berger, Ramya Ramaswami, Caren G. Solomon, and Jeffrey M. Drazen. Air Pollution Still Kills. *New England Journal of Medicine*, 376(26):2591–2592, 2017.
- Michela Bia, Carlos A. Flores, Alfonso Flores-Lagunes, and Alessandra Mattei. A Stata package for the application of semiparametric estimators of doseresponse functions. *The Stata Journal*, 14(3): 580–604, 2014.
- Matthew Cefalu, Francesca Dominici, Nils Arvold, and Giovanni Parmigiani. Model averaged double robust estimation. *Biometrics*, 73(2):410–421, 2017.
- Lisa M Chiodo, Sandra W Jacobson, and Joseph L Jacobson. Neurodevelopmental effects of postnatal lead exposure at very low levels. *Neurotoxicology and Teratology*, 26:359–371, 2004.
- Michael J. Daniels, Francesca Dominici, Jonathan M. Samet, and Scott L. Zeger. Estimating Particulate Matter-Mortality Dose-Response Curves and Threshold Levels: An Analysis of Daily Time-Series for the 20 Largest US Cities. *American Journal of Epidemiology*, 152(5):397–406, 2000.
- Michael J Daniels, Francesca Dominici, Scott L Zeger, and Jonathan M Samet. The National Morbidity, Mortality, and Air Pollution Study. Part III: PM10 concentration-response curves and thresholds for the 20 largest US cities. *Research report (Health Effects Institute)*, (94 Pt 3):1–21; discussion 23–30, may 2004. ISSN 1041-5505.
- Qian Di, Lingzhen Dai, Yun Wang, Antonella Zanobetti, Christine Choirat, Joel D. Schwartz, and Francesca Dominici. Association of Short-term Exposure to Air Pollution With Mortality in Older Adults. *Journal of the American Medical Association*, 318(24):2446, dec 2017a.

- Qian Di, Yan Wang, Antonella Zanobetti, Yun Wang, Petros Koutrakis, Christine Choirat, Francesca Dominici, and Joel D. Schwartz. Air Pollution and Mortality in the Medicare Population. *New England Journal of Medicine*, 376(26):2513–22, 2017b.
- Francesca Dominici, Michael Daniels, Scott L Zeger, and Jonathan M Samet. Air Pollution and Mortality: Estimating Regional and National Dose-Response Relationships. *Journal of the American Statistical Association*, 97(457):100–111, 2002. ISSN 0162-1459. doi: 10.1198/016214502753479266.
- Sorina E. Eftim, Jonathan M. Samet, Holly Janes, Aidan McDermott, and Francesca Dominici. Fine Particulate Matter and Mortality: A Comparison of the Six Cities and American Cancer Society Cohorts With a Medicare Cohort. *Epidemiology*, 19(2):209–216, mar 2008. ISSN 1044-3983. doi: 10.1097/EDE.0b013e3181632c09.
- Reza Fazel, Harlan M. Krumholz, Yongfei Wang, Joseph S. Ross, Jersey Chen, Henry H. Ting, Nilay D. Shah, Khurram Nasir, Andrew J. Einstein, and Brahmajee K. Nallamothu. Exposure to Low-Dose Ionizing Radiation from Medical Imaging Procedures. *New England Journal of Medicine*, 361(9):849–857, aug 2009.
- Andrew Gelman and Donald B. Rubin. Inference from Iterative Simulation Using Multiple Sequences. *Statistical Science*, 7(4):457–511, 1992.
- Andrew Gelman, Jessica Hwang, and Aki Vehtari. Understanding predictive information criteria for Bayesian models. *Statistics and Computing*, 24(6):997–1016, nov 2014. ISSN 0960-3174. doi: 10.1007/s11222-013-9416-2.
- Usha S Govindarajulu, Elizabeth J Malloy, Bhaswati Ganguli, Donna Spiegelman, and Ellen A Eisen. The comparison of alternative smoothing methods for fitting non-linear exposure-response relationships with Cox models in a simulation study. *The international journal of biostatistics*, 5(1):Article 2, 2009. ISSN 1557-4679. doi: 10.2202/1557-4679.1104.
- P J Green. Reversible jump Markov chain Monte Carlo computation and Bayesian model determination. *Biometrika*, 82:711–732, 1995.
- Trevor Hastie. gam: Generalized Additive Models, 2017.
- Trevor Hastie and Robert Tibshirani. Generalized Additive Models. *Statistical Science*, 1(3):297–318, 1986.
- Trevor Hastie and Robert Tibshirani. Varying-Coefficient Models. *Journal of the Royal Statistical Society. Series B*, 55(4):757–796, 1993.
- W K Hastings. Monte Carlo sampling methods using Markov chains and their applications. *Biometrika*, 57(1), 1970. doi: 10.1093/biomet/57.1.97/284580.
- Keisuke Hirano and Guido W Imbens. The Propensity Score with Continuous Treatments \*. 2004.
- Todd A Jusko, Charles R Henderson, Bruce P Lanphear, Deborah A Cory-Slechta, Patrick J Parsons, and Richard L. Canfield. Blood Lead Concentrations < 10 g/dL and Child Intelligence at 6 Years of Age. *Environmental health perspectives*, 116(2):243–8, feb 2008.

- Edward H. Kennedy, Zongming Ma, Matthew D. McHugh, and Dylan S. Small. Non-parametric methods for doubly robust estimation of continuous treatment effects. *Journal of the Royal Statistical Society: Series B (Statistical Methodology)*, 79(4):1229–1245, sep 2017. ISSN 13697412. doi: 10.1111/rssb.12212.
- Xavier De Luna, Ingeborg Waernbaum, and Thomas S. Richardson. Covariate selection for the nonparametric estimation of an average treatment effect. *Biometrika*, 98(4):861–875, 2011. ISSN 00063444. doi: 10.1093/biomet/asr041.
- Sarah Jane Mackenzie Ross, Chris Ray Brewin, Helen Valerie Curran, Clement Eugene Furlong, Kelly Michelle Abraham-Smith, and Virginia Harrison. Neuropsychological and psychiatric functioning in sheep farmers exposed to low levels of organophosphate pesticides. *Neurotoxicology and teratology*, 32(4):452–9, 2010.
- David Madigan, Jeremy York, and Denis Allard. Bayesian Graphical Models for Discrete Data. *International Statistical Review*, 63(2):215–232, 1995. ISSN 03067734. doi: 10.2307/1403615.
- Nicholas Metropolis, Arianna W Rosenbluth, Marshall N Rosenbluth, Augusta H Teller, and Edward Teller. Equation of State Calculations by Fast Computing Machines. *The Journal of Chemical Physics*, 21(6):1087–1092, 1953. doi: 10.1063/1.439486.
- National Research Council. *Health Risks from Exposure to Low Levels of Ionizing Radiation: BEIR VII Phase 2*. The National Academies Press, Washington, D.C., mar 2006.
- Jerzy Neyman. On the Application of Probability Theory to Agricultural Experiments. Essay on Principles. Section 9. *Statistical Science*, 5(4):465–480, 1923.
- Adrian E. Raftery. Bayesian Model Selection in Social Research. *Sociological Methodology*, 25: 111–163, 1995.
- Adrian E Raftery, David Madigan, and J Hoeting. Bayesian model averaging for linear regression models. *Journal of the American Statistical Association*, 92(437):179–191, 1997. ISSN 0162-1459. doi: 10.1080/01621459.1997.10473615.
- Donald B. Rubin. Estimating causal effects of treatments in randomized and nonrandomized studies. *Journal of Educational Psychology*, 66(5):688–701, 1974. ISSN 0022-0663. doi: 10.1037/h0037350.
- Donald B Rubin. Randomization Analysis of Experimental Data: The Fisher Randomization Test Comment. *Source Journal of the American Statistical Association*, 75(371):591–593, 1980.
- Joseph Schafer. `causaldrf`: Tools for Estimating Causal Dose Response Functions, 2015.
- Martin Scholze, Wolfgang Boedeker, Michael Faust, Thomas Backhaus, Rolf Altenburger, and L Horst. A general best-fit method for concentration-response curves and the estimation of low-effect concentrations. *Environmental Toxicology and Chemistry*, 20(2):448–457, 2001.
- Joel Schwartz, Francine Laden, and Antonella Zanobetti. The Concentration-Response Relation between PM<sub>2.5</sub> and Daily Deaths. *Environmental Health Perspectives*, 110(10):1025–1029, 2002.
- Gavin Shaddick, Duncan Lee, James V. Zidek, and Ruth Salway. Estimating exposure response functions using ambient pollution concentrations. *Annals of Applied Statistics*, 2(4):1249–1270, 2008. ISSN 19326157. doi: 10.1214/08-AOAS177.

- Liuhua Shi, Antonella Zanobetti, Itai Kloog, Brent A Coull, Petros Koutrakis, Steven J Melly, and Joel D Schwartz. Low-Concentration PM<sub>2.5</sub> and Mortality: Estimating Acute and Chronic Effects in a Population-Based Study. *Environmental health perspectives*, 124(1):46–52, jan 2016. ISSN 1552-9924. doi: 10.1289/ehp.1409111.
- Mark J Van Der Laan, Eric C Polley, and Alan E Hubbard. Super Learner. *Statistical Applications in Genetics and Molecular Biology*, 6(1), 2007.
- Ron Van Der Oost, Jonny Beyer, and Nico P E Vermeulen. Fish bioaccumulation and biomarkers in environmental risk assessment: a review. *Environmental Toxicology and Pharmacology*, 13:57–149, 2003.
- Stijn Vansteelandt, Maarten Bekaert, and Gerda Claeskens. On model selection and model misspecification in causal inference. *Statistical methods in medical research*, 21(1):7–30, 2012. ISSN 1477-0334. doi: 10.1177/0962280210387717.
- Chi Wang, Giovanni Parmigiani, and Francesca Dominici. Bayesian Effect Estimation Accounting for Adjustment Uncertainty. *Biometrics*, 68(3):661–671, 2012.
- Chi Wang, Francesca Dominici, Giovanni Parmigiani, and Corwin Matthew Zigler. Accounting for uncertainty in confounder and effect modifier selection when estimating average causal effects in generalized linear models. *Biometrics*, 71(3):654–665, 2015.
- Sumio Watanabe. Asymptotic Equivalence of Bayes Cross Validation and Widely Applicable Information Criterion in Singular Learning Theory. *Journal of Machine Learning Research*, 11: 3571–3594, 2010.
- Ander Wilson and Brian J. Reich. Confounder selection via penalized credible regions. *Biometrics*, 70(4):852–861, 2014.
- Antonella Zanobetti and Joel Schwartz. Particulate air pollution, progression, and survival after myocardial infarction. *Environmental health perspectives*, 115(5):769–75, may 2007. ISSN 0091-6765. doi: 10.1289/ehp.9201.
- Scott L Zeger, Francesca Dominici, Aidan McDermott, and Jonathan M Samet. Mortality in the Medicare population and chronic exposure to fine particulate air pollution in urban centers (2000–2005). *Environmental health perspectives*, 116(12):1614–9, dec 2008. ISSN 0091-6765. doi: 10.1289/ehp.11449.
- Corwin M. Zigler and Francesca Dominici. Point: Clarifying Policy Evidence With Potential-Outcomes Thinking Beyond Exposure-Response Estimation in Air Pollution Epidemiology. *American Journal of Epidemiology*, 180(12):1133–1140, 2014.